



DISTRIBUTION STATEMENT A
Approved for public release
Distribution Unlimmed

**INVESTIGATING SORBENT GEOMETRY
RESPONSE SURFACES
FROM SORPTION RATE DATA**

THESIS

H. Michael Harrison, Major, USAF

AFIT/GOA/ENV/98M-01

19980409 022

DTIC QUALITY INSPECTED

**DEPARTMENT OF THE AIR FORCE
AIR UNIVERSITY
AIR FORCE INSTITUTE OF TECHNOLOGY**

Wright-Patterson Air Force Base, Ohio

AFIT/GOA/ENV/98M-01

**INVESTIGATING SORBENT GEOMETRY
RESPONSE SURFACES
FROM SORPTION RATE DATA**

THESIS

H. Michael Harrison, Major, USAF

AFIT/GOA/ENV/98M-01

Approved for public release; distribution unlimited

The views expressed in this thesis are those of the author and do not reflect the official policy or position of the United States Air Force, Department of Defense, or the U. S. Government

**INVESTIGATING SORBENT GEOMETRY RESPONSE
SURFACES FROM SORPTION RATE DATA**

THESIS

Presented to the Faculty of the Graduate School of Engineering
of the Air Force Institute of Technology
Air University
In Partial Fulfillment of the
Requirements for the Degree of
Master of Science in Operations Analysis

H. Michael Harrison, B.S., M.A.

Major, USAF

March, 1998

Approved for public release; distribution unlimited

THESIS APPROVAL

Student: Major H. Michael Harrison, B.S., M.A.

Class: GOA-98M

Thesis Title: Investigating Sorbent Geometry Response
Surfaces From Sorption Rate Data

Approved

Committee

Date

Edward Heyse

6 MAR 98

Maj Edward Heyse, PhD
(Committee Chairman)

Glenn Bailey

6 March 1998

Lt Col Glenn Bailey, PhD
(Committee Member)

D L Coulliette

6 MAR 98

Lt Col David L. Coulliette, PhD
(Committee Member)

ACKNOWLEDGMENTS

I would like to express my sincere thanks to my faculty and advisors, Lt Col Glenn Bailey and Maj Ed Heyse. Without their support, my research would not have been feasible. Maj Heyse's knowledge of sorption and diffusion models enabled me to gain an understanding of this research area that I didn't think was possible. He made himself available for frequent office visits and always took the time and effort to answer my questions. His quick review of the chapter I was currently working on allowed me to keep the writing process moving quickly.

Lt Col Bailey's Response Surface Methodology course and personal knowledge of the subject proved to be an invaluable resource for this work. I am also grateful to Lt Col Dave Coulliette for introducing me to this research topic, as well as his work writing the FORTRAN subroutine for the gamma distribution. Many thanks to Dr. Mark Goltz for taking the time to read and comment on the rough draft. His inputs gave the thesis greater clarity. This research effort was possible through the continued support of the Air Force Office of Scientific Research (AFOSR).

Finally, and most importantly, I want to thank my family. Without your prayers, support, understanding, and sacrifice of quality family time, I could never have completed this assignment. Thank you for your confidence in my ability.

Mike Harrison

TABLE OF CONTENTS

	Page
ACKNOWLEDGEMENTS	iii
List of Figures	vi
List of Tables.....	vii
ABSTRACT	viii
I. INTRODUCTION	1
II. LITERATURE REVIEW	4
Sorption Processes	4
Sorption Models	6
Dealing with Heterogeneity.....	8
Desirable Distribution Characteristics.....	12
Candidate Distributions	13
III. METHODOLOGY	17
Data Sets	17
Composite Sorbent Particle	18
Response Surface Methodology	21
Process	22
Screening	23
Design of Experiments	24
Method of Steepest Descent	26
IV. RESULTS AND ANALYSIS	28
Introduction	28
Size Dependence of D_{eff}	28
RSM and Statistical Distributions	31
Radial Geometry Function	31
Gamma Density Function.....	34
Borden Data Set.....	36
V. SUMMARY AND CONCLUSIONS	39

APPENDIX A: Borden Soil Data Set.....	41
APPENDIX B: Mika's (1997) Even Data Set, Condition 5	42
APPENDIX C: MSS Models.....	46
APPENDIX D: Details of RSM Procedure for Radial Geometry Function.....	71
REFERENCES	75
VITA	79

List of Figures

	Page
1. Multiple Sites in Parallel (MSP) Model (Heyse, 1994)	10
2. Multiple Sites in Series (MSS) Model (Heyse, 1994).....	11
3. Gamma Probability Density Function	14
4. Lognormal Probability Density Function.....	15
5. Weibull Probability Density Function.....	16
6. Particle Distributions.....	19
7. Composite Sorbent Particle, Different K_p and D_{eff}	21
8. Graphical Representation of Response Process	22
9. Sample Minimum Response Surface.....	27
10. Loss of Data Points and Relation to D_{eff}	31
11. Radial Geometry Function SSE Response Surface From Regression Equation	32
12. Radial Geometry Function SSE Surface From MSS Model Data.....	33
13. Radial Geometry Function Contour Plot of \log (SSE).....	33
14. Gamma Density Function SSE Surface From MSS Model Data	35
15. Borden Soil SSE Surface From MSS Model Data	37

List of Tables

	Page
1. Borden Site Data (adapted from Ball and Roberts, 1991a, b)	17
2. Synthetic Soil Statistics (de Venoge, 1996)	18
3. 2^2 Factorial Design	24
4. Diffusion Coefficients Adjusted for Bead Size Variance.....	30

**INVESTIGATING SORBENT GEOMETRY RESPONSE
SURFACES FROM SORPTION RATE DATA**

ABSTRACT

AFIT/GOA/ENV/98M-01

Sorption and desorption of hydrophobic organic compounds (HOCs) into soil particles occurs at Air Force contamination sites. Long-term desorption extends clean up time, costing billions. Accurately modeling desorption will reduce costs and improve clean up designs. State of the art models depict soil as uniform spherical particles which lose the effect of longer sorption path lengths. An alternate approach, the multiple sites in series (MSS) model, describes the sorption capacity of a mixture of soil particle sizes and shapes using a composite particle defined by a two parameter statistical distribution. When the MSS model uses a general radial geometry function as the statistical distribution, unique parameters can not be fit to laboratory experimental data. This research employs response surface methodology (RSM) to investigate the nonunique parameter model deficiency. Analysis shows that the response surface for the general radial geometry function is a trough with no unique minimum. A unique minimum is found when the statistical distribution is changed to a gamma distribution.

I. INTRODUCTION

Hydrophobic organic compounds contaminate groundwater at many hazardous waste sites. These chemicals threaten the health and safety of those where the groundwater is used for water supply. A great deal of time, money, and research is being applied to clean the chemicals from the groundwater, but the efforts are not always successful.

To make remediation efforts more successful, research is focusing on the modeling of solute transport. The transport process can be classified into three broad categories: 1) solute transfer between phases (sorption, dissolution), 2) spatial transport of a solute within a fluid (advection, dispersion, diffusion), and 3) chemical change of solutes (biodegradation). This research effort examines solute transfer between phases.

The purpose of a model simulating solute transport is to predict the contaminant concentration at a particular time and point in space (Konikow, 1981). However, there are so many parameters to estimate that the task is difficult for one model to be able to compute the values effectively. For this and other reasons, several models are used to calculate parameter estimates that are used in the overall calculation of a contaminant concentration.

A chemical contaminant in water will migrate toward locations where it is less concentrated. This process is known as *diffusion*. In soil systems where the concentrations change with time, Fick's second law is applied. In one dimension, Fick's second law is written as

$$\frac{\partial C}{\partial t} = D \cdot \frac{\partial^2 C}{\partial x^2}$$

where *C* = concentration,
t = time, and
D = diffusion coefficient.

In soil systems, diffusion will not proceed as fast as in water because the solute must travel longer distances due to the tortuous paths around solids. To account for this, an effective diffusion coefficient, D_{eff} , is used, which includes a measure of the effect of the shape of the flowpath followed by the molecules (Fetter, 1992). Calculation of the effective diffusion coefficient is simplified by using data obtained in laboratory experiments. Computer models can fit D_{eff} coefficients using known concentrations from experimental data over time.

Heyse's (1994) multiple sites in series (MSS) model will fit several parameters to experimental data, one of which is D_{eff} . The MSS model can also fit geometry parameters to data sets, which allows characterization (size, shape) of a composite soil particle. Previous research has found two problems with the MSS model, namely, that the D_{eff} parameter depends on the size of the synthetic sorbent spheres used in laboratory experiments, and the geometry parameters found for mixtures of particle sizes are not unique.

In order for modeling to be useful, consistent results should be obtained. The size dependent D_{eff} coefficients are unexpected. For a given system, the diffusion coefficient should generally not be dependent on the size of the particles for correctly defined geometries. An error is occurring that causes the size dependent D_{eff} coefficients. This error could involve the assumption of Fickian diffusion, the laboratory data, the composite shape approach, or even the model code itself, just to name a few of the possible sources. If the MSS model is to be used to help predict contaminant concentrations, it must also be able to predict unique geometry parameters for a given soil system so that different systems can be characterized in laboratory experiments.

To improve the MSS model, this research will examine and explain the size dependence of the D_{eff} coefficients. The utility of the model will increase if the diffusion

coefficients it predicts are within a range of expected values and also constant for a given sorbent.

The second objective of this research is to characterize the nature of the geometry parameters' response surface. The sum of squares for error (SSE) is calculated between known data and model predictions by the MSS model. Response surface methodology will be used to show the shape of the SSE response surface formed by the two input geometry parameters. The shape of the surface may explain why there is no unique *best fit* pair of parameters. Finally, this effort will investigate another function in the MSS model to construct the SSE surface and determine if a unique pair of geometry parameters can be found.

II. LITERATURE REVIEW

The most common hazardous contaminants at Air Force waste sites are hydrophobic organic compounds (HOCs), such as chlorinated solvents and aircraft fuel components. Current research is concentrating on how to model the movement of these chemicals in order to determine the best remediation measures. For this research to be effective, knowledge of the physical, chemical, and biological processes occurring to the contaminants in groundwater is essential.

Sorption Processes

Sorption is an important physical-chemical process and is the means by which chemicals associate with solid phases (Schwarzenbach *et al.*, 1993). The generic term *sorption* includes both adsorption and absorption. Adsorption is the accumulation occurring at an interface while absorption is the partitioning between two phases. For absorption, the equilibrium partition coefficient (K_p) quantifies the solute distribution between the liquid and solid phases. If a soil has a significant natural organic carbon content (≥ 0.1 percent), sorption by the soil organic matter (SOM) dominates all other HOC sorption processes (Karickhoff, 1981).

Sorption is a complex process that is receiving much attention in the literature. Better understanding of this process will allow improved model construction and remediation design, as well as improved knowledge of waste site contaminant transport. Currently, sorption is modeled with equilibrium or nonequilibrium models, each with their own assumptions and limitations.

A common assumption made in modeling sorption is that of local equilibrium. The local equilibrium assumption (LEA) states that the solute is at equilibrium between all phases

at any point in space and is used to simplify the transport equations (Valocchi, 1986; Goltz and Oxley, 1991). According to the LEA, the process of a contaminant partitioning between sorbed and dissolved phases is instantaneous. However, there are numerous cases where equilibrium conditions do not prevail in the subsurface. Nonequilibrium sorption of HOCs at the grain scale exists because mass transfer between moving groundwater and SOM is governed by diffusion, a slow process compared to advective transport with groundwater flow (Brusseau and Rao, 1989; Brusseau *et al.*, 1991).

The two most accepted theories of HOC sorption nonequilibrium are intraorganic matter diffusion (IOMD) and retarded intraparticle diffusion (RIPD). IOMD involves absorption (partitioning) of a chemical species within the matrix of SOM (Chiou *et al.*, 1979; Chiou *et al.*, 1983). RIPD involves aqueous-phase diffusion and sorption of contaminant species within the microscopic pores of mineral grains (Wu and Gschwend, 1986; Ball and Roberts, 1991b).

Nonequilibrium sorption is important because it results in both earlier arrival and longer tailing of solutes moving past a location in space. There are several important implications as sorption mass transfer slows: 1) the duration of exposure to a solute increases, potentially increasing health risks, 2) more time is required for engineered restoration activities, increasing clean up costs, and 3) solutes spend more time in the sorbed phase where they are probably not available for biodegradation (Scow and Alexander, 1992), possibly decreasing the effectiveness of natural attenuation or intrinsic remediation.

Sorption Models

Sorption kinetics are modeled in one of three ways, depending on the assumptions made and the level of mathematical detail desired. If equilibrium can be assumed, the rate of change of sorbed phase contaminant is proportional to the rate of change of aqueous phase contaminant, shown in equation (1)

$$\frac{dS}{dt} = K_p \frac{dC}{dt} \quad (1)$$

where S = *sorbed phase concentration*,
 K_p = *equilibrium partition coefficient, and*
 C = *solute concentration.*

Nonequilibrium models employ either first- or second-order approximations of diffusion (Parker and Valocchi, 1986; Wu and Gschwend, 1986; Brusseau and Rao, 1989; Ball and Roberts, 1991b). The first-order model uses a first-order mass transfer expression to describe the sorption domain as a discrete distribution. This model is described mathematically using equation (2)

$$\frac{dS}{dt} = k_2 (K_p C - S) \quad (2)$$

where k_2 = *first-order mass transfer rate.*

The first-order description of the sorption domain is highly simplified which allows computational ease, but makes correlations for new combinations of chemicals and solids from previously fit combinations difficult (Wu and Gschwend, 1986). The second-order description is based on molecular (Fickian) diffusion and phase partitioning. The time rate of change of sorbed compound per unit volume is expressed using Fick's second law of diffusion in radial coordinates, most often employing a spherical geometry. This radial diffusion is described by equations (3) through (7)

$$\frac{\partial S}{\partial t} = \frac{\theta_s}{\rho} \frac{\partial \bar{C}_s}{\partial t} \quad (3)$$

$$\bar{C}_s = \frac{3}{R^3} \int_0^R r^2 C_s dr \quad (4)$$

$$\frac{\partial C_s}{\partial t} = \frac{D_{eff}}{r^2} \frac{\partial}{\partial r} \left(r^2 \cdot \frac{\partial C_s}{\partial r} \right) \quad (5)$$

$$C_s (r = R) = K_p C \quad (6)$$

$$\left. \frac{\partial C_s}{\partial r} \right|_{r=0} = 0 \quad (7)$$

where D_{eff} = *effective diffusion coefficient*,
 C_s = *volumetric concentration in soil organic matter at position r and time t*,
 \bar{C}_s = *average sorbed phase concentration*,
 R = *radius of sphere*,
 ρ = *soil bulk density*,
 θ_s = *volumetric water content*.

As with all mathematical modeling, these equations contain limitations. The first-order model requires the assumptions that 1) all sorption sites are located at the same path length, and 2) concentration gradients are linear between the sorbed and aqueous phases. This is not always the case. The first-order model does a poor job at reproducing long-term slow desorption, and mass transfer rate coefficients have been experimentally found to depend on groundwater velocity. Also, first-order models usually assume a single mass transfer rate coefficient for the sorption and desorption of contaminants to and from natural sediments (Brusseau and Rao, 1989). This assumption often causes model failure when simulating sorptive mass transfer under changing solvent velocities (Brusseau, 1992; Heyse, 1994; Heyse *et al.*, 1997) or extended contamination contact times (Karickhoff and Morris, 1985; Connaughton *et al.*, 1993; Young and Ball, 1995; Culver *et al.*, 1997). First-order models can not deal with heterogeneity either. Some research has accounted for

heterogeneity by using multiple first-order sites (Connaughton *et al.*, 1993; Heyse, 1994; Culver *et al.*, 1997; Haggerty and Gorelick, 1995). Although the multiple-particle class formulation of the first-order mass transfer model allows for variations in sorption rate and equilibrium, measuring these parameters is not experimentally possible (Pedit and Miller, 1994). The first-order models are approximating diffusion, but a second-order model will always approximate diffusion more closely.

The second-order model presented above assumes that all sorption sites are distributed as uniform spheres. This is certainly not the case because natural sorbents are heterogeneous mixtures with complex geometries (Brewer, 1964; Weber *et al.*, 1992). Also, since the diffusion model requires the calculation of solute concentrations at all radial coordinates in the sphere, it is mathematically more complex than the first-order approach.

Dealing with Heterogeneity

The assumption of homogeneous spherical particle geometries as usually employed in second-order diffusion based models is unrealistic. SOM is very heterogeneous, being comprised of various molecular sizes and densities. Schnitzer (1978) and Stevenson (1982) report SOM to be a flexible, cross-linked, branched, amorphous, polyelectrolytic polymeric substance with various distributions of grain sizes. A soil's diagenetic history involves the physical and chemical changes occurring during and after formation. Weber *et al.* (1992) and Young and Weber (1995) report significant differences in soil based on diagenetic age of the soil, and hence, the SOM contained in it. Older SOM has a condensed, almost crystalline structure that is significantly more hydrophobic, causing slower diffusion. On the other hand, younger SOM has a rubbery, more open structure that is less hydrophobic and allows for faster sorption. Clearly SOM is not homogeneous.

To improve sorption mass transfer models, the effects of heterogeneity are usually included by using one of three methods. The first technique is to model all soil particles as an equivalent sphere. The equivalent sphere can be determined in one of two ways. The first is to find the equivalent sphere that gives the same specific interfacial area as the aggregated sorbent. The second is to select a sphere of mean radius for the soil under consideration and fit a diffusion coefficient. The mean radius is often selected as the sieve size through which fifty percent of the mass will pass. The spherical diffusion model can then be fit to data by modifying the diffusion coefficient. However, by describing concentrations at all path lengths in the sphere, all models require a significant amount of computational effort to solve (requires larger, slower models). Another problem that arises is that the effect of longer path lengths are lost (Haggerty and Gorelick, 1995). Likewise, the multiple-particle class formulation of the Fickian diffusion model can only address variability down to the individual particle scale, which assumes an individual particle to be homogeneous and does not allow for intraparticle variations in sorption rate and equilibrium (Pedit and Miller, 1994). These models are also very complex.

The second method used to account for heterogeneity involves using the continuum of compartments concept proposed by Connaughton *et al.* (1993). The multiple sites in parallel (MSP) model, as shown in Figure 1, employs multiple compartments. Each compartment is defined by a first-order mass transfer rate. Connaughton *et al.* (1993) and Culver *et al.* (1997) use a gamma distribution to describe the mass transfer rates, while Heyse (1994) and Culver *et al.* (1997) use a lognormal distribution, all with varying degrees of success. MSP models of this type are not computationally difficult, but analytical solutions are only possible for the simplest of boundary conditions. The biggest problem

found is that changing the boundary conditions results in different distributions (model parameters) (Connaughton *et al.*, 1993; Heyse, 1994).

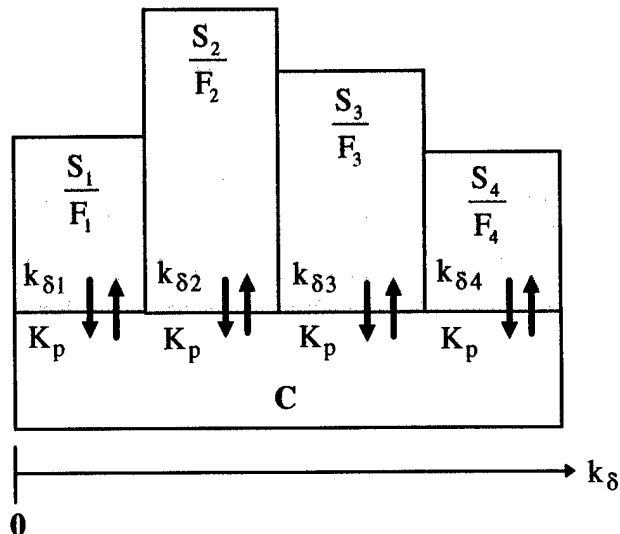


Figure 1, Multiple Sites in Parallel (MSP) Model (Heyse, 1994)

A variation of the MSP model was described by Haggerty and Gorelick (1995). Their multirate model is different from others in that instead of a statistical distribution of rate coefficients, the size and rate constants are derived so that they give results identical to diffusion-based models. Multiple sites or compartments each have their own first-order rate. The rates in each compartment can be fixed so that the model gives the same results as a layered, cylindrical, or spherical diffusion model. Different particle sizes and shapes can be modeled simultaneously by weighting each particle size/shape by its fraction of sorbing capacity. A potential drawback is that the solution is derived using a uniform concentration as the initial condition in the sorbed phase. This initial condition may result in different solutions when the boundary conditions change.

The third method of dealing with heterogeneity in diffusion models is to include all geometric shape descriptions in one composite (but nonspherical) shape. Heyse (1994) introduced the multiple sites in series (MSS) model as depicted in Figure 2. It is simply a finite difference solution to the diffusion equation into any geometry as described

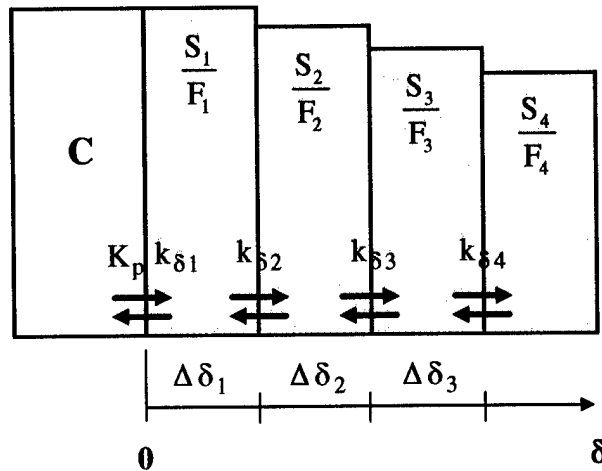


Figure 2, Multiple Sites in Series (MSS) Model (Heyse, 1994)

by a frequency distribution of sorption capacities along a single diffusion path. de Venoge (1996) and Mika (1997) used the geometric function given in equation (8) to describe a composite particle's geometry. By including the shape factor (λ) in the frequency distribution, different particle geometries can be described.

$$f(\delta) = \begin{cases} \frac{\lambda+1}{R^{\lambda+1}} (R-\delta)^\lambda & 0 \leq \delta \leq R \\ 0 & \text{otherwise} \end{cases} \quad (8)$$

where $f(\delta)$ = frequency distribution representing sorption capacity,
 λ = shape factor,
 R = maximum diffusion path length, and
 δ = variable diffusion path length.

A uniform coating has $\lambda = 0$, $\lambda = 1$ describes a cylinder, and a spherical particle results from

$\lambda = 2$. Equation (8) represents the cross-sectional area normalized to the volume of the sorbent over the range from $\delta = 0$ (sorbent / water interface) to $\delta = R$ (center of the particle). Note that the diffusion path length δ is measured from the liquid interface in equation (8), but equations (3) - (7) measure radius from the center of the particle. Equation (8) makes the diffusion path length computationally easier to use. It describes a distribution of sorption sites along a diffusion path length. Additionally, higher order geometries can be represented by increasing the shape factor. Higher shape factors result in a majority of sorption sites at short diffusion path lengths, but with some sites at very long path lengths. The description of diffusion path lengths with a frequency distribution that includes a shape factor is intuitively appealing since it can account for the complex geometries associated with natural solid phases. However, as shown by Mika (1997), the disadvantage of this distribution is that for shape factors (λ) much greater than two, the distribution gives a nonunique solution.

Desirable Distribution Characteristics

To expand on the work of de Venoge (1996) and Mika (1997), this thesis tests the gamma distribution for use in the MSS model. For a statistical distribution to be desirable, there should be no more than two fitting parameters. This prevents the model from becoming too complex. These fitting parameters need to describe the composite geometry of soil particles using an $f(\delta)$ distribution. The shape of the distribution must provide high frequencies at low δ values to account for a rapid uptake of solute and a long tail to describe rate-limited sorption over extended time periods.

The distribution must also be unique for a given sorbent. The distribution evaluated at zero is the specific interfacial area, as defined below

$$f(0) = a = \frac{\text{interfacial area}}{\text{volume}}$$

The first normalized moment (mean) of the distribution is the average diffusion path length,

$\bar{\delta}$, where $\bar{\delta} = \frac{\int_0^\infty \delta \cdot f(\delta) d\delta}{\int_0^\infty f(\delta) d\delta} = \int_0^\infty \delta \cdot f(\delta) d\delta$, since the denominator is one. Mika (1997)

found that for any best fit geometry, the value $D \frac{a}{\bar{\delta}}$ was constant.

Candidate Distributions

Several statistical distributions meet the above criteria. This research effort tests the gamma distribution for use in the MSS model and evaluates this distribution for uniqueness of fit using response surface methodology (RSM). See Hastings and Peacock (1975), or Law and Kelton (1991) for more detailed discussions of statistical distributions. The lognormal and Weibull density functions are included here because they represent the general shape of a desired distribution. Although this thesis does not test their use in the MSS model, they could have computational advantages and should be the subject of future research.

The gamma distribution is depicted below in Figure 3, where $\text{gamma}(x, \alpha)$ is the form of the curves that are shown. Figure 3 only displays changes in the shape parameter, α , which demonstrates the variability of the gamma distribution. It is characterized by a shape parameter, α , and a scale parameter, β , both of which must be greater than zero. As is seen in the figure, when the shape parameter α is less than one, the density takes on infinite values as x approaches zero. For certain types of soil geometries, this may prove beneficial, since the mean of the diffusion path lengths may be located at various values of δ . As is shown in the figure, the gamma distribution can take on many shapes, depending on the values of α

and β . The exponential distribution is a special case of the gamma distribution, as is seen by $\text{gamma}(x, 1)$ in Figure 3.

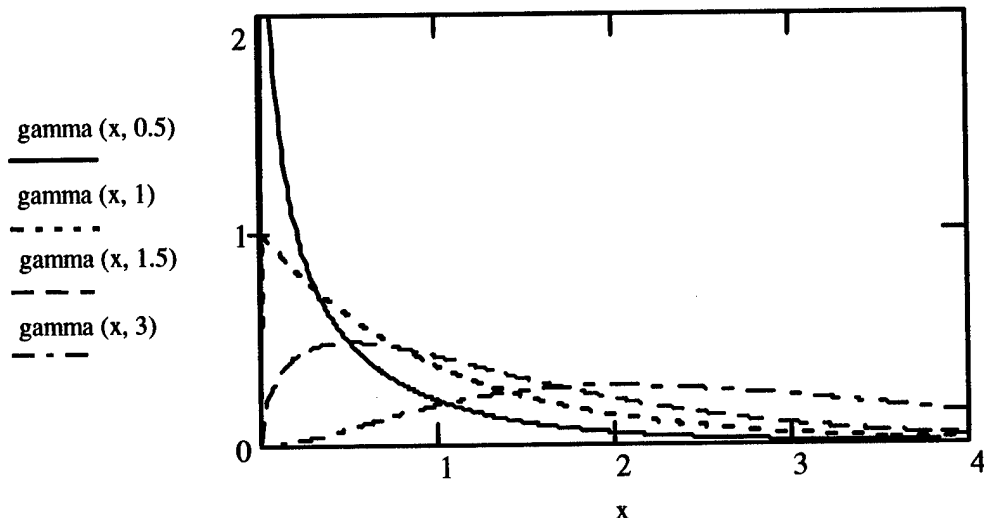


Figure 3, Gamma Probability Density Function

The gamma density function is given by equation (9)

$$f(x) = \frac{\beta^{-\alpha} x^{\alpha-1} e^{-x/\beta}}{\Gamma(\alpha)} \quad (9)$$

where $\Gamma(\alpha) = \int_0^{\infty} e^{-u} u^{\alpha-1} du$, the mean is given by $\alpha \cdot \beta$ and the variance by $\alpha \cdot \beta^2$.

Figure 4 shows the lognormal distribution. The curves on the graph are of the form $\text{lognorm}(x, \mu, \sigma)$. This distribution is also characterized by a shape parameter, σ , and a scale parameter, μ , where $\sigma > 0$ and $-\infty < \mu < \infty$. Notice in Figure 4 that lognormal curves can be shifted away from the origin. As with the gamma distribution, this may prove beneficial for certain types of soil geometries.

The lognormal density function is given in equation (10)

$$f(x) = \frac{1}{x\sqrt{2\pi\sigma^2}} \exp\left[\frac{-(\ln x - \mu)^2}{2\sigma^2}\right] \quad (10)$$

with mean $\mu \cdot \exp(0.5 \cdot \sigma^2)$ and variance $\mu^2 \cdot (\sigma^2 + 1) \cdot \exp(2\sigma^2)$.

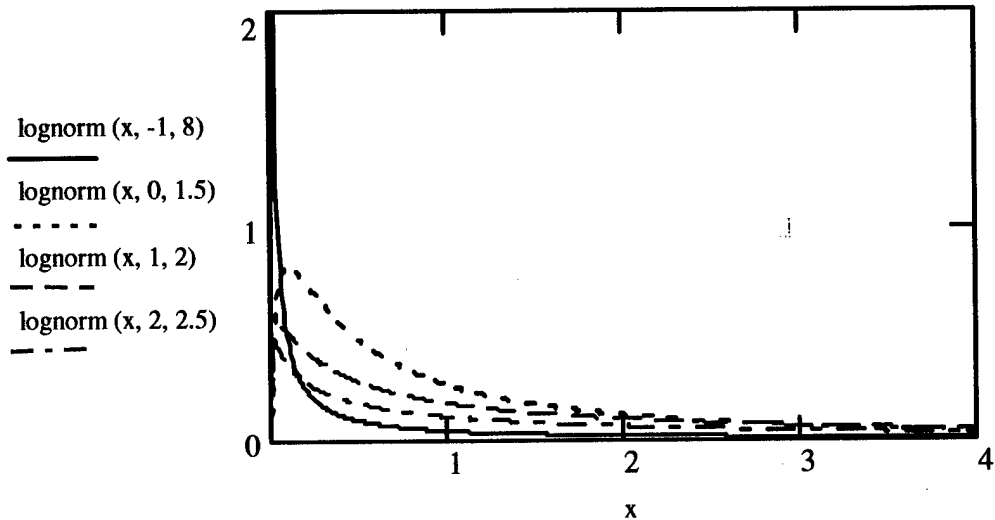


Figure 4, Lognormal Probability Density Function

The last distribution to be considered is the Weibull, shown in Figure 5. Graphed curves are of the form $\text{Weibull}(x, \alpha)$ where only changes in the shape parameter, α , are demonstrated.

As with the gamma distribution, if the shape parameter is less than one, the density takes on infinite values as x approaches zero. Certain types of soil geometries may require this capability. Also note that as the shape parameter increases, the Weibull distribution begins to resemble a normal distribution. The Weibull distribution has shape and scale parameters, α and β respectively, both greater than zero. The Weibull density function is given by equation (11)

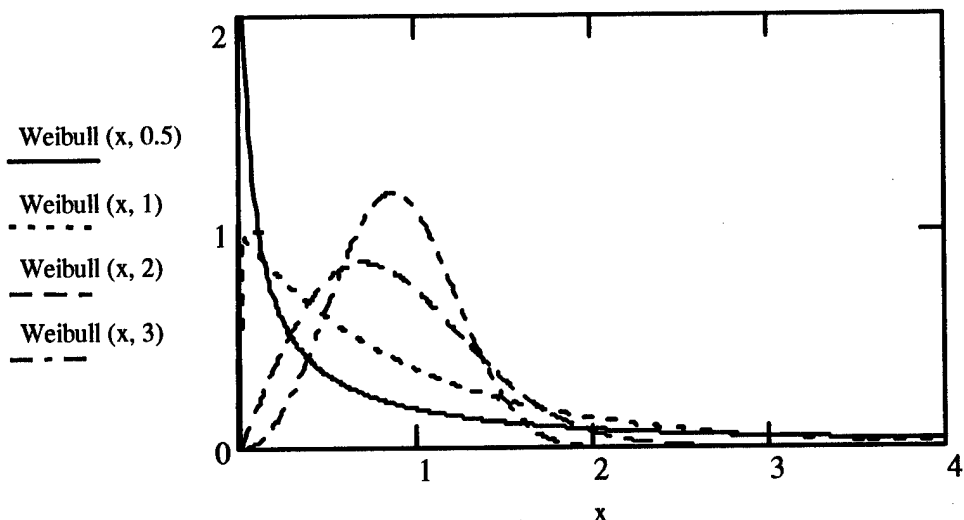


Figure 5, Weibull Probability Density Function

$$f(x) = \alpha \beta^{-\alpha} x^{\alpha-1} \exp\left(-\left(\frac{x}{\beta}\right)^\alpha\right) \quad (11)$$

with mean $\beta \cdot \Gamma\left(\frac{\alpha+1}{\alpha}\right)$ and variance $\beta^2 \left\{ \left[\Gamma\left(\frac{\alpha+2}{\alpha}\right) \right] - \left[\Gamma\left(\frac{\alpha+1}{\alpha}\right) \right]^2 \right\}$, with the gamma

function as previously defined.

III. METHODOLOGY

Data Sets

This research compares the ability of Heyse's (1994) MSS model to describe sorption by heterogeneous mixes of sorbents as representative, composite particles using two different functions. The general radial geometry function (equation 8) and the gamma density function (equation 9) are used to describe the sorbent capacity of a representative composite particle along a diffusion path length. These models are tested using two data sets.

One data set is a simulation of sorptive uptake of tetrachloroethene (PCE) by a sandy aquifer material from Borden, ON in a batch system. This simulation is created using the model of Haggerty and Gorelick (1995) and based on Borden soil characteristics as defined by Ball and Roberts (1991a, b), shown in Table 1. The data set produced from this simulation is presented in Appendix A. It is used as input for the MSS model as a natural sorbent.

Table 1, Borden Site Data (adapted from Ball and Roberts, 1991a, b)

Particle Fraction	Mass Fraction, F	R, mm	K _p , mL/g	D _s , cm ² /sec $\times 10^{11}$
1	0.0091	0.6	8	11.2
2	0.0524	0.3	2.9	8.28
3	0.163	0.16	1.2	5.89
4	0.257	0.11	0.55	3.27
5	0.315	0.075	0.3	5.29
6	0.615	0.048	0.26	3.92
7	0.0341	0.03	0.82	1.26
Composite	0.9956		0.727	3.39
Bulk	1	0.11	0.74	3.39

The second data set consists of sorption of anthracene in a methanol/water solution by paraffin beads conducted by Mika (1997). The manufacture of the paraffin beads, a synthetic sorbent created for the study of multisite sorption models, is outlined by de Venoge (1996). The size and consistency of these paraffin beads is shown in Table 2. Mika (1997) uses these same beads to conduct sorption/desorption experiments in a batch system on two different mixtures of paraffin bead sizes. The even mix contained 7 large, 12 medium, and 23 small beads. The uneven mix contained 2 large, 5 medium, and 53 small beads. The equilibrium partition coefficient (K_p) is estimated to be 9.35 mL/g by linear regression ($R^2 = 0.9997$). Mika's (1997) even data set is included in Appendix B.

Table 2, Synthetic Soil Statistics (de Venoge, 1996)

Statistics	Sphere Size		
	Large	Medium	Small
Average Mass (g)	0.09253	0.05511	0.02808
Standard Deviation	0.00342	0.00158	0.00110
Maximum	0.09740	0.05972	0.03010
Minimum	0.08610	0.05232	0.02491
Count	21	36	70
Max Radius (cm)	0.297	0.249	0.1997
D_{eff} (cm ² /s $\times 10^{-8}$)	2.12	2.01	1.96

Composite Sorbent Particle

Natural sorbent particles are heterogeneous; the approach of this research is to incorporate heterogeneity into a composite sorbent particle. This is illustrated for two separate cases: 1) homogeneous material (same K_p , D_{eff}), heterogeneous shape, and 2) heterogeneous material and shape.

Case 1: Homogenous material, heterogeneous shape. Assume each particle class (size and shape) can be defined by its mass fraction, F_j , its radius, R_j , and its shape factor, λ_j . Since each mass fraction has the same K_p and D_{eff} , the two distributions can be added to form

one composite sorbent particle distribution, as shown in Figure 6, where $f_j(\lambda, \delta)$ is as defined in equation (8).

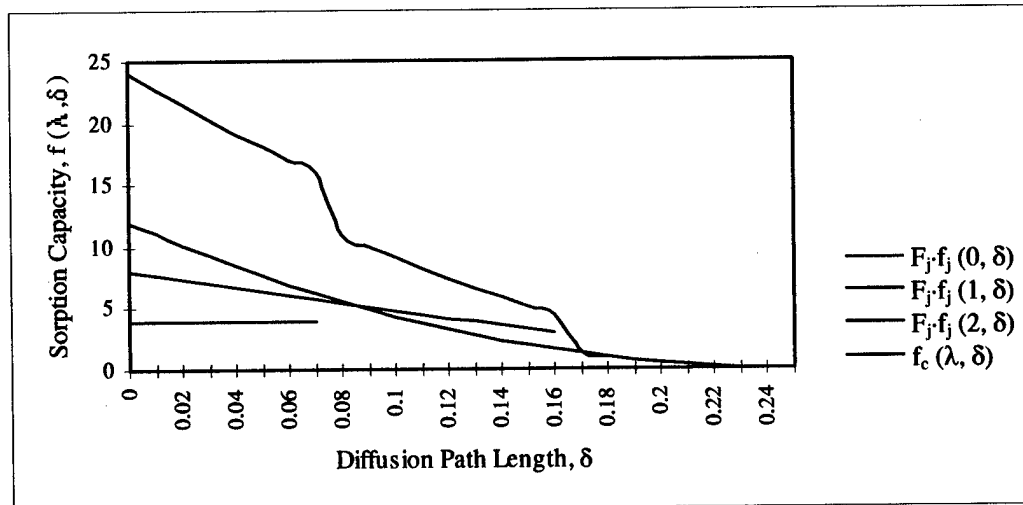


Figure 6, Particle Distributions

The distribution of the composite particle $f_c(\delta)$ is defined in equation (12)

$$f_c(\delta) = \sum_j F_j \cdot f_j(\delta) \quad (12)$$

Once the composite distribution is determined, a composite particle can be obtained by using the equations for specific interfacial area (a) and average diffusion path length ($\bar{\delta}$) from Chapter II.

Case 2: Heterogeneous material and shape. The sorption characteristics (K_p , D_{eff}) of natural sorbents will vary along with particle size and shape. Individual particles must be normalized to an average K_p and representative D_{eff} so a single composite particle can be defined. The average K_p is obtained by

$$K_{p, \text{avg}} = \frac{\sum_j M_j \cdot K_{p,j}}{\sum_j M_j} \quad (13a)$$

$$= \sum_j F_j \cdot K_{p,j} \quad (13b)$$

Several variables need to be transformed. A prime symbol will denote a *virtual* particle. The virtual mass and mass fractions are defined in equations (15) and (16).

$$M_j' \Rightarrow M_j \cdot \frac{K_{p,j}}{K_{p, \text{avg}}} \quad (14)$$

$$F_j' \Rightarrow F_j \cdot \frac{K_{p,j}}{K_{p, \text{avg}}} \quad (15)$$

In order for the mass flux of the real and virtual particles to remain the same

$$\left[\frac{a}{\bar{\delta}} \right]' \cdot D_0 = \left[\frac{a}{\bar{\delta}} \right] \cdot D_{\text{eff},j} \quad (16)$$

where D_0 is a representative diffusion coefficient.

The specific interfacial area (a) and the average diffusion path length ($\bar{\delta}$) are defined by

$$a_j = f_j(0) = \frac{\lambda_j + 1}{R_j} \quad (17)$$

$$\bar{\delta}_j = \int_0^{R_j} \delta \cdot f_j(\delta) d\delta = \frac{R_j}{\lambda_j + 2} \quad (18)$$

The particle shape must be maintained in the virtual particle, so $\lambda_j = \lambda'_j$. By inserting equations (17) and (18) into equation (16) and simplifying, the virtual radius, R'_j , is shown in equation (19)

$$R'_j = R_j \cdot \sqrt{D_0 / D_{eff,j}} \quad (19)$$

The virtual particles are illustrated in Figure 7. Since $K_{p,avg}$ and D_0 are the same for each particle, a composite sorbent particle distribution, $f_c(\delta)$, is obtained using equation (12) as in case 1.

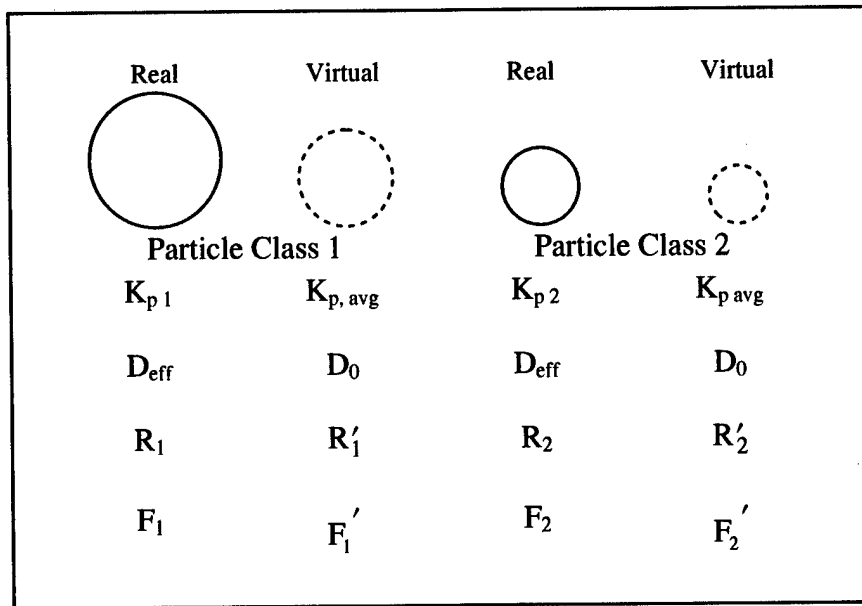


Figure 7, Composite Sorbent Particle, Different K_p and D_{eff}

Response Surface Methodology

RSM comprises mathematical and statistical techniques to develop, improve, or optimize various processes (Myers and Montgomery, 1995). The input variables, called *independent variables*, are under the control of the researcher, while the output variables, or the *response*, is a function of the process under study. This concept is shown graphically in Figure 8, where ξ_k represents the process inputs and $E(y)$ is the expected value of the response, y .

Process

In the context of Figure 8 and RSM, the MSS model is the process under study, or the *black box*. The MSS program takes in a number of variables and fits either a diffusion coefficient (D_{eff}), a shape factor and diffusion path length (λ, R), or gamma function parameters (α, β) by minimizing the sum of squares for error (SSE). By varying the input parameters, this research examines the response surface of SSE with the original radial geometry function and with a gamma distribution for $f_c(\delta)$ in the model code to determine if a unique solution exists.

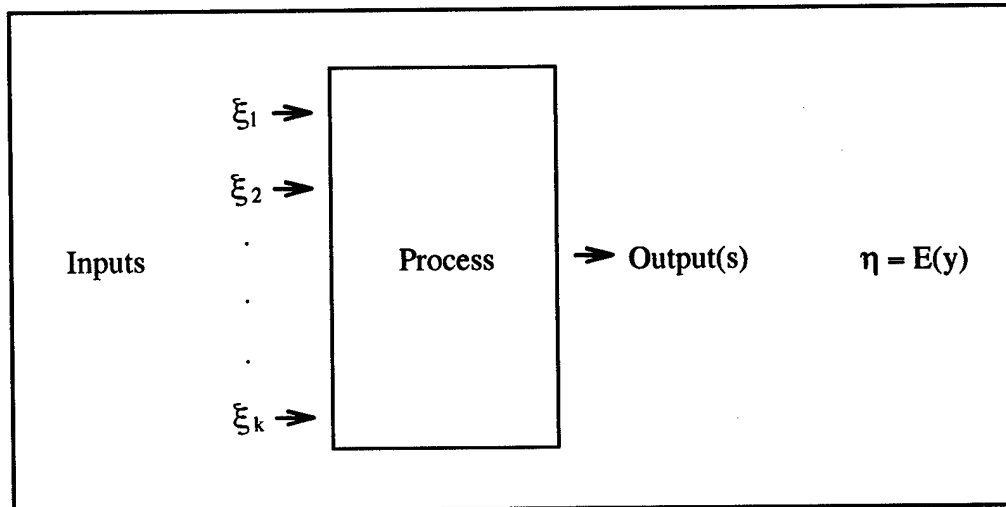


Figure 8, Graphical Representation of Response Process

A numerical model to describe sorption and desorption with perturbations (liquid phase added or removed during the course of experimentation) is used to predict sorption behavior and compare predictions of the MSS model to the data sets. The governing equation is given by equation (20)

$$V_L \frac{\partial C}{\partial t} + M \frac{\partial S}{\partial t} = 0 \quad (20)$$

where V_L = *volume of liquid phase*,
 M = *mass of paraffin*, and
 $\frac{\partial S}{\partial t}$ is defined by the *MSS model*.

At some time t , liquid is removed and may be added to the reactor. The new boundary conditions are defined by

$$S_j(t) = S_{j-1}(t)$$

$$V_j \cdot C_j(t) = V_{j-1} \cdot C_{j-1}(t) - V_R(t) \cdot C_{j-1}(t) + V_A(t) \cdot C_j(t)$$

$$V_j = V_{j-1} - V_R(t) + V_A(t)$$

where j = *boundary condition*,
 t = *time boundary condition changes*,
 V_R = *volume of liquid removed*,
 V_A = *volume of liquid added*, and
 $C_j(t)$ = *concentration of liquid during boundary condition j at time t* .

The model features a finite difference approach employing implicit time and central space differencing. Two different versions are used, featuring the composite particle described by the general radial geometry function and by the gamma density function. Both models calculate SSE between the model prediction and a data set, and are included in Appendix C. In order to determine the nature of the response surface, there are several phases of the RSM procedure to be implemented.

Screening

Normally, the first phase of RSM involves a screening process to determine which of the independent variables significantly influence the response. In this research, however, there are at most two independent variables to be examined. Therefore, screening experiments will not be necessary. The radial geometry function uses λ and R as the

independent variables, while the gamma density function uses α and β . For both functions, the response is SSE.

Design of Experiments

The second phase of RSM uses the most significant variables to form a first-order approximation of the SSE response. To form this approximation, factorial designs are typically employed. Factorial designs are used to study the joint effects of several independent variables on a response (Montgomery, 1976). By using two levels of the independent variables, or *factors*, a 2^k factorial design is created where there are k total factors being studied. The factors in this study, λ and R or α and β , are referred to as factors A and B, respectively. Each factor will be set to a low and a high level, resulting in a 2^2 factorial design, where all possible combinations of low and high levels result in four runs, or design points. Each run of the MSS model produces a response, labeled y_1 through y_4 , as shown in Table 3.

Table 3, 2^2 Factorial Design

Run #	Treatment Combination	Factorial Effect				Response, y SSE
		I	A	B	AB	
1	A low, B low	+	-	-	+	y_1
2	A high, B low	+	+	-	-	y_2
3	A low, B high	+	-	+	-	y_3
4	A high, B high	+	+	+	+	y_4

Using the designed experiments from Table 3, a linear approximation of the functional relationship between A, B, and y is produced. This is accomplished with regression analysis, a statistical technique for modeling the response as a linear combination of various forms of the input variables and their interactions. Before performing the regression analysis, the input variables are *standardized*, or coded, using equation (21)

$$x_i = \frac{X_i - X_{i0}}{S_i} \quad (21)$$

where x_i = new coded variable,
 X_i = original uncoded variable,
 X_{i0} = center of range for variable X_i , and
 S_i = half of the range for variable X_i .

This transforms the variable range to -1 and +1, corresponding to the levels under consideration, low and high. The reason for coding is two-fold. First, it increases the computational ease and accuracy of the model coefficients since the $X'X$ matrix for the 2^2 design will have some of the off-diagonal elements equal to zero. Second, the coefficient estimates in the model are easier to interpret because the parameter estimates of the linear model are uncorrelated and therefore provide statistically independent test statistics (Khuri and Cornell, 1987).

The general first-order regression model is $y = X\beta + \epsilon$, where the bold symbols indicate a vector. Errors associated with this model fall into two categories: 1) random errors, which produce the variance, σ^2 , arise from measurement errors of the process under study (included in ϵ), and 2) systematic errors, or bias errors, of the type $X\cdot b - E(y)$ (Myers and Montgomery, 1995). Since the MSS model is deterministic, there are no random errors, leaving only bias errors in the regression model (first- or second-order). In order to obtain the minimum bias, a minimum bias design will be used in this research.

To construct a minimum bias design, the factorial design points are pushed closer to the center of the design. Using the coded values from equation (21), the new points would be at $\pm\sqrt{1/3}$ instead of ± 1 . By shrinking the overall design region, model bias and variance are minimized as opposed to the usual criterion of minimizing only the model variance.

Method of Steepest Descent

Using the first-order response model of SSE obtained through regression analysis, a gradient search technique called the method of steepest descent (MOSD) iteratively determines the next region for experimentation. MOSD is continued until the response (SSE) no longer decreases (or decreases only slightly). The first order response is then augmented with interaction effects and the overall model fit is checked. If the correlation coefficient (R^2) is not satisfactory, a second order response is fit. At this point the two-level factorial design is augmented to include center points in order to test for curvature. The central composite design (CCD) is typically used for fitting a second-order response. To make the CCD a minimum bias design, the axial points are placed at ± 1 and the nonaxial points are placed at $\pm\sqrt{1/2}$. Thus all design points are maintained on a circle of radius equal to one, shrinking the design region under investigation and reducing the bias.

The MSS model will be tested with the radial geometry function and the gamma density function to get a picture of the response surface in the minimum SSE region, if it exists. The hypothesis is that changing from the radial geometry function to the gamma density function in the MSS model will find an actual minimum SSE rather than a locus of points of relatively constant SSE. This will improve the capability of the MSS model to predict contaminant concentrations in soil systems. A notional response surface is given in Figure 9, which shows a minimum response (at least locally).

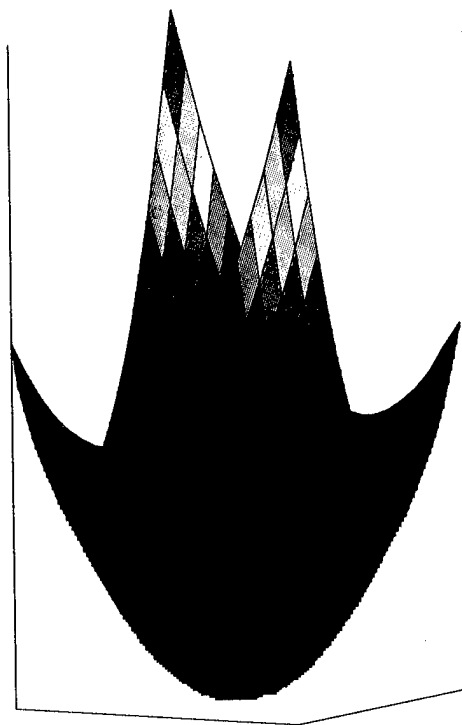


Figure 9, Sample Minimum Response Surface

IV. RESULTS AND ANALYSIS

Introduction

The purpose of this thesis is to improve sorption mass transfer models by using a composite geometry to describe a heterogeneous mixture of sorbent particles. The improvement comes from describing a composite particle geometry using a statistical distribution to preserve all diffusion path lengths. By doing so, current models can better predict long-term contaminant residence times.

The first objective is to attempt to explain the size dependence of fitted values of the diffusion coefficient, D_{eff} , from paraffin data obtained by de Venoge (1996) and Mika (1997).

The second objective is to investigate a statistical distribution to obtain a unique fit of two parameters that describe the composite geometry. Mika (1997) found that fitting the general radial geometry function yielded nonunique parameters. The measure of fit is sum of squares for error (SSE). Can a minimum SSE be found for a pair of fitting parameters, or is there only a range of values available?

Size Dependence of D_{eff}

The MSS model predicts different diffusion coefficients in two separate research efforts. de Venoge (1996) observed that the fitted D_{eff} depended on the size of the paraffin bead being modeled, which was then attributed to not presoaking the paraffin beads in a methanol/water solution. Mika (1997) presoaked the paraffin beads and obtained different diffusion coefficients. However, these new coefficients still depend on the paraffin bead size. de Venoge (1996) shows that sphere mass is normally distributed but the variance of the sphere masses is dependent on the sphere size. A possible explanation is that the

variation of sphere mass (and therefore sphere size) causes the size dependence of fitted D_{eff} coefficients.

Mathematically, the quantity $D \cdot a / \bar{\delta}$ describes the mass transfer rate constant. Fitting one or more of these parameters results in adjusting parameters so $D \cdot a / \bar{\delta}$ remains constant. For a given solvent/sorbate/sorbent system, the diffusion coefficient should be constant if the particle size and shape are correctly described.

However, if the geometry (defined by the size index) is improperly defined, the fitting program adjusts the diffusion coefficient to compensate and maintain mass balance. In this study, beads are described as uniformly sized spheres when they actually should have been described as normally distributed sized spheres.

The diffusion coefficient for a composite shape representing normally distributed spheres can be estimated by

$$D_{ND} = D_{sphere} \cdot \frac{(a/\bar{\delta})_{sphere}}{(a/\bar{\delta})_{ND}}$$

where $ND = \text{normally distributed}$.

Using the sphere statistics in Table 2, a distribution of radii is obtained for each sphere size. This statistical description is used to estimate the size index of the composite shape of the large, medium, and small beads using the procedure for a homogeneous material, heterogeneous shape described in Chapter III.

The results of this effort are presented in Table 4. The difference in size indices between the composite shape and the nominal uniform sphere shape can not explain the size dependence of the fitted D_{eff} coefficients.

Table 4, Diffusion Coefficients Adjusted for Bead Size Variance

Bead Size	Fitted D_{eff} (spherical)	Size Index (spherical)	Adjusted D_{eff} (spherical)	Size Index (composite)
Large	2.12	136.0	2.06	139.8
Medium	2.01	193.5	1.94	200.3
Small	1.96	300.9	1.89	313.4

Another possible explanation for the size dependence of D_{eff} has to do with the frequency and spacing of samples. During all experiments, samples are taken at the same time for all sizes of sorbents within a given condition. But since the smaller beads have a faster rate of sorption (high surface to volume ratio), the samples show parts of the rate curve closer to equilibrium than would the same samples for the large beads.

In order to examine the spacing of samples, data points could be removed from a large bead data set before using it in the MSS model to calculate D_{eff} . This would be similar to an experiment with smaller beads where samples are not taken until the system is closer to equilibrium. Figure 10 illustrates the effect of omitting data points from a sorption experiment by Mika (1997) using large beads. When early samples are deleted from the data set, the fitted D_{eff} coefficient decreases. Deletion of later samples has little effect on D_{eff} indicating the importance of early measurements when concentration changes rapidly with time and where most of the overall concentration change occurs. This is the factor that explains the size dependence of D_{eff} . It is therefore important to capture the early concentration changes in order to obtain an accurate D_{eff} .

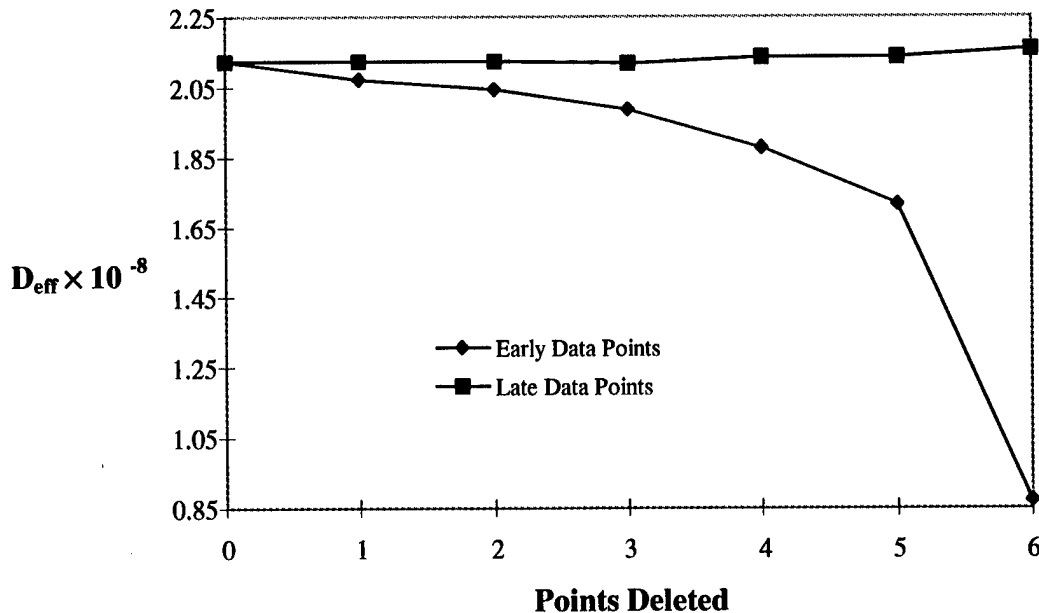


Figure 10, Loss of Data Points and Relation to D_{eff}

RSM and Statistical Distributions

In order to better visualize the problem of fitting nonunique shape and size parameters with the radial geometry function, RSM is used to characterize the SSE response surface using Mika's (1997) even size bead mix data set found in Appendix B. A detailed description of the RSM procedure for the radial geometry function is in Appendix D.

Radial Geometry Function

The augmented first-order design results in the following regression equation with $R^2 = 0.7945$

$$\hat{y} = -0.4195 + 0.2585 \cdot \lambda + 2.1298 \cdot R - 1.2165 \cdot \lambda \cdot R$$

Since all p-values indicate that no terms are significant, a second-order response surface is fit. The resulting regression equation is

$$\hat{y} = 0.10856 + 0.05997 \cdot \lambda - 1.2371 \cdot R + 0.0400 \cdot \lambda^2 - 0.9831 \cdot \lambda \cdot R + 6.71595 \cdot R^2$$

with a correlation coefficient (R^2) of 0.9694. Figure 11 is a plot of the regression equation.

All terms are left in the equation since it results in virtually the same surface as with only the significant terms. Note that in order to remain in the trough region of the surface, and

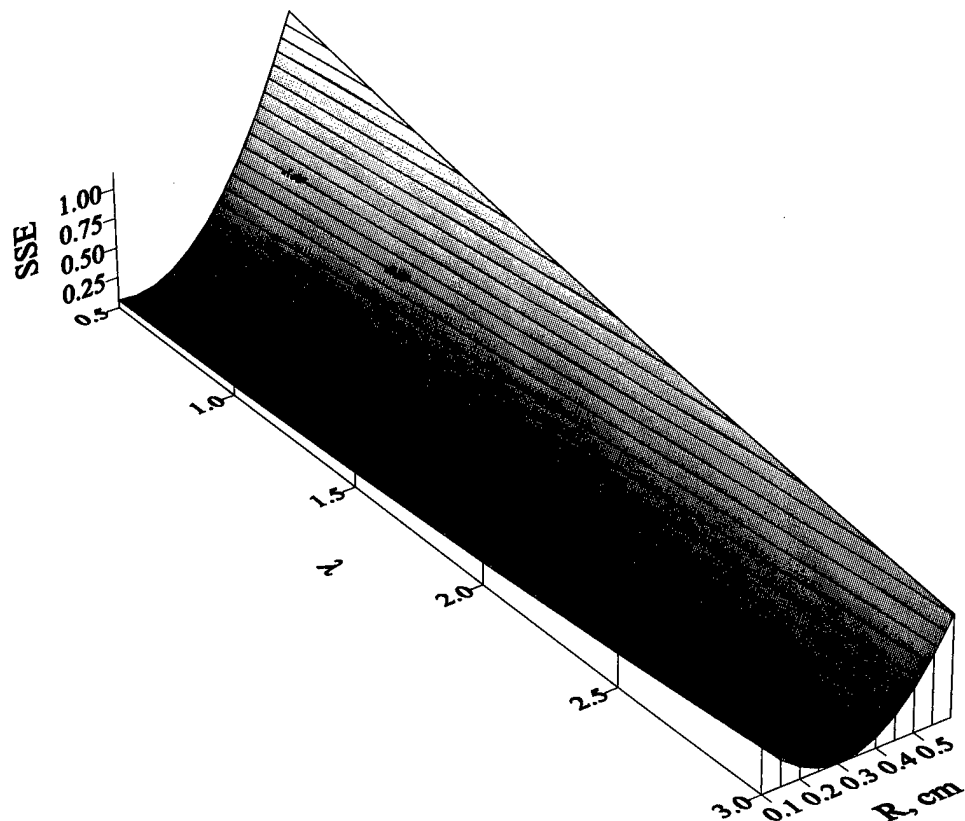


Figure 11, Radial Geometry Function SSE Response Surface From Regression Equation

hence near a minimum SSE, λ and R both increase as the trough moves away from the origin. Figure 12 is a plot of the true surface using actual data from the MSS model. The figure shows the nature of the true surface encountered, demonstrating that there is no unique

best fit pair of λ and R . Both figures demonstrate that as λ and R increase, the width of the trough grows. This is another limitation of the radial geometry function, since real soil systems are probably characterized by composite shape factors, $\lambda \gg 2$. Figure 13 is a plot of $\log(\text{SSE})$ contours, allowing a better visualization of the trough. Figure 13 shows that the trough widens as the surface extends from the origin. Although not visible from this plot, the SSE values also decrease slightly as the trough widens.

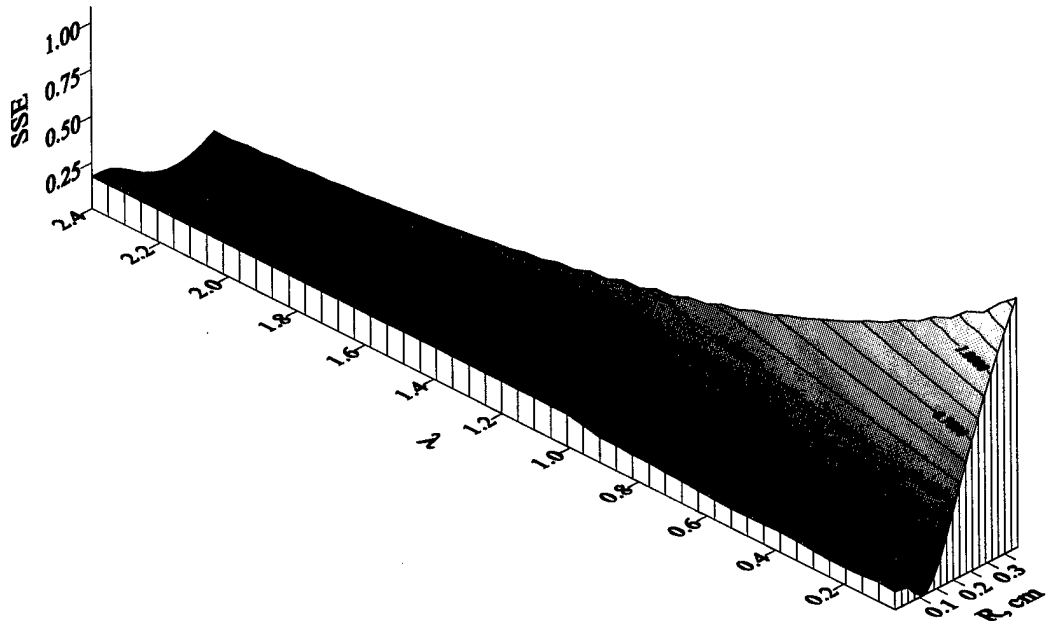


Figure 12, Radial Geometry Function SSE Surface From MSS Model Data

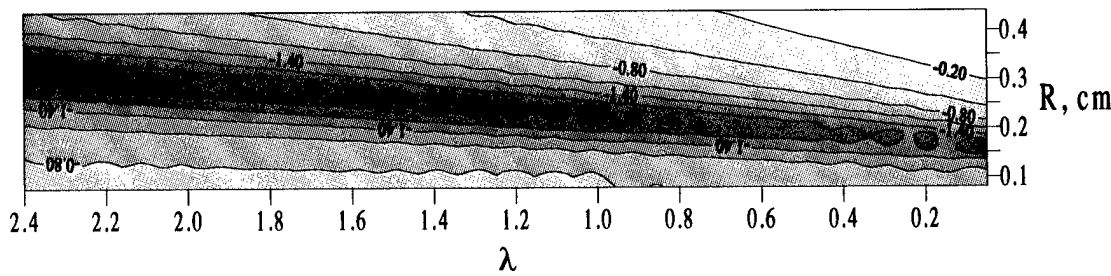


Figure 13, Radial Geometry Function Contour Plot of $\log(\text{SSE})$

Gamma Density Function

After changing the radial geometry function in the MSS model code to a gamma density function, Mika's (1997) even size bead mix data set is again used to evaluate the SSE response with RSM. By using a gamma density function instead of the radial geometry function, a unique pair of fitting parameters is found. To correspond with the gamma function, these parameters are named α and β . The shape parameter, α , controls the shape of the gamma function. Increasing it has an effect similar to decreasing λ in the radial geometry function. The scale parameter, β , is similar to R in the radial geometry function, although β is dimensionless. The radial geometry function is intuitively appealing since R can be visualized as the actual particle radius in centimeters and $\lambda = 0, 1$, or 2 represents a layer, cylinder, or sphere, respectively, as mentioned in Chapter II. Unfortunately, α and β do not have this same physical interpretation.

The first-order augmented design for the gamma function MSS model is

$$\hat{y} = 0.7476 - 0.8629 \cdot \alpha - 8.4792 \cdot \beta + 9.860 \cdot \alpha \cdot \beta$$

with a corresponding R^2 of 0.9271. At first glance, this model appears to be adequate.

However, the p-values for all parameter estimates are ≥ 0.293 , indicating a better model is available. The second-order response function is

$$\hat{y} = 1.5096 - 1.9220 \cdot \alpha - 15.6135 \cdot \beta + 0.6155 \cdot \alpha^2 + 9.8676 \cdot \alpha \cdot \beta + 41.4526 \cdot \beta^2$$

where $R^2 = 0.9999$ and all p-values are < 0.0001 . Figure 14 is a plot of the SSE values calculated by the MSS model using the gamma density function. A plot of the above regression equation looks similar, but does not show the minimum as clearly as the plotted values of α , β , and SSE in Figure 14. This plot clearly demonstrates that a unique minimum

pair of fitting parameters exists for the MSS model when using the gamma density function. The area of the minimum seems quite large in Figure 14 since $0.84 \leq \alpha \leq 0.95$ and $0.075 \leq \beta \leq 0.095$ will result in approximately the same SSE. However, α and β can range from zero to infinity for the gamma function. Therefore, the area of the minimum in Figure 14 is relatively small.

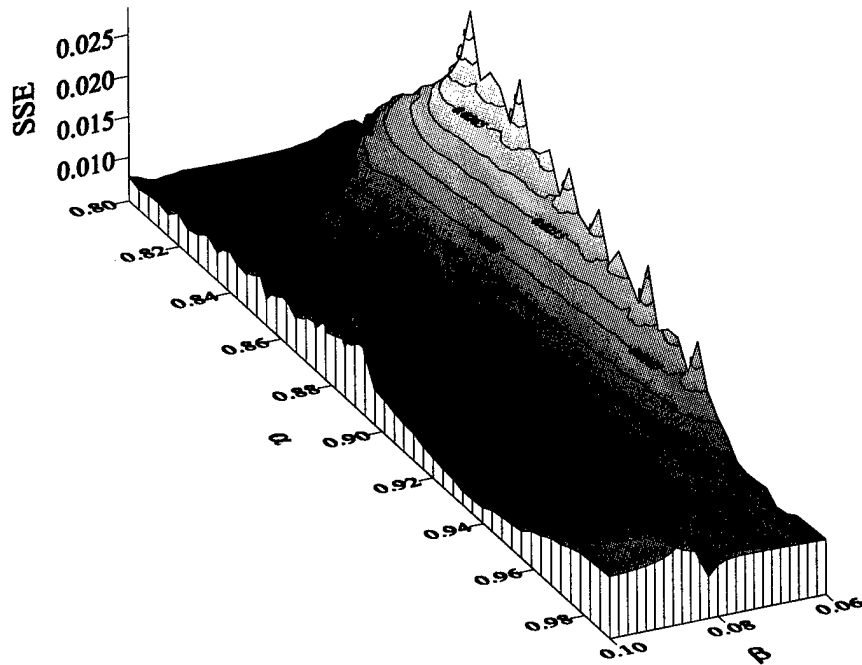


Figure 14, Gamma Density Function SSE Surface From MSS Model Data

There is a definite advantage of the gamma MSS model over the radial geometry version of the MSS model. The gamma MSS model will obtain a unique pair of fitting parameters for a given soil mixture. The radial geometry MSS model will not fit unique pairs of parameters, only a unique size index. If unique parameters for both size and shape of composite sorbent particles can be fit from data, these parameters can characterize natural sorbents (soil systems) more thoroughly than the single parameter, size index. Even if the

size and shape parameter have no physical interpretation as in the radial geometry function, different soil systems can be compared based on unique fitting parameters.

Real soil systems are heterogeneous mixes of particle sizes that are only roughly approximated by even or uneven mixes of paraffin beads. Since the even mix of paraffin beads in Mika's (1997) data has a unique minimum pair of fitting parameters, the obvious test of the new gamma MSS model is to see if it will find a unique pair of fitting parameters for a real soil system.

Borden Data Set

The Borden data set as described in Chapter III is based on real soil. Appendix A contains a simulated data set for the MSS model based on the Borden soil. Using this simulated data, the RSM procedure is applied to the gamma function version of the MSS model to see if it will find a unique pair of fitting parameters for real soil.

The augmented first-order design for the Borden data is

$$\hat{y} = 0.5618 - 3.7512 \cdot \alpha - 0.1993 \cdot \beta + 3.0773 \cdot \alpha \cdot \beta$$

The correlation coefficient for this equation is only 0.007, while the unaugmented first-order design has $R^2 = 0.8508$. The lower R^2 is due to the curvature of the response surface and indicates the need for a second-order response to be fit. The second-order response surface equation is

$$\hat{y} = -13.193 - 12.1518 \cdot \alpha + 16.854 \cdot \beta + 44.7592 \cdot \alpha^2 + 2.7823 \cdot \alpha \cdot \beta - 5.2112 \cdot \beta^2$$

with $R^2 = 0.9137$. Figure 15 is a plot of the MSS model SSE responses with the Borden data set.

For a real soil data set, the gamma version of the MSS model finds an actual minimum pair of fitting parameters. From Figure 15 it appears that there are actually two

regions where a minimum can occur. However, the actual data points show that the true minimum is within the larger of the two circular areas. The figure just doesn't include enough lines to show this fact. The significant point is that the gamma MSS model locates a unique minimum for real soil.

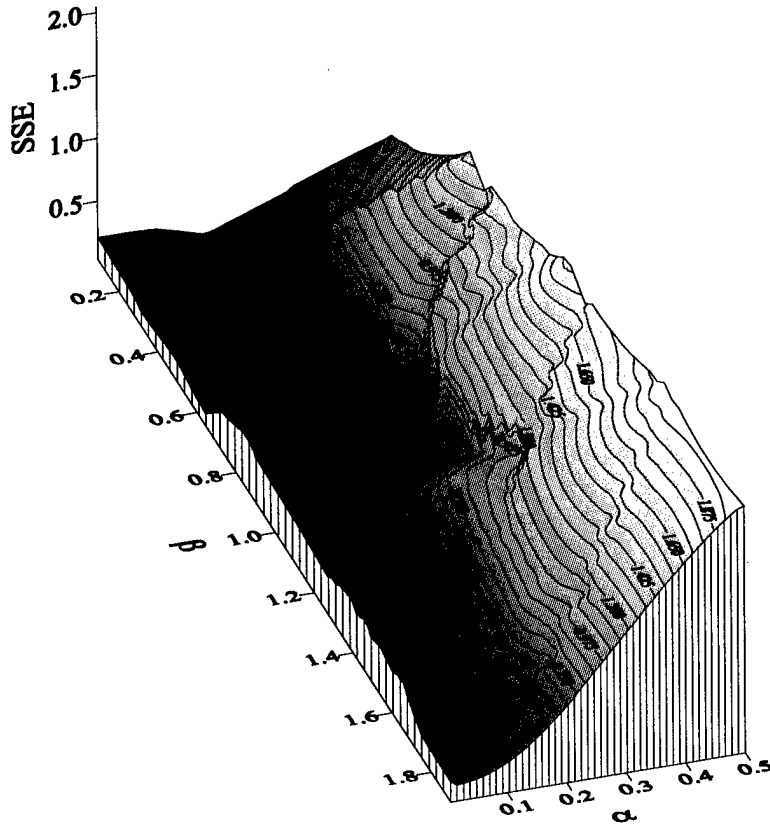


Figure 15, Borden Soil SSE Surface From MSS Model Data

With the Borden soil data set, $\alpha \approx 0.1$ in the gamma MSS model, and $\lambda \approx 8.0$ in the radial geometry MSS model. This value of α is very low considering that there is no upper limit to the range for α . For Mika's (1997) even mix, $\alpha \approx 0.9$ in the gamma MSS model and the corresponding shape factor in the radial geometry function is approximately 2.7. The significance is that in the radial geometry function, the shape factor increases for real soil and

has the range to do so. For the gamma MSS model, this range is not available since the shape factor decreases for real soil and has a lower limit of zero. The small available range for the shape factor in the gamma MSS model may be the reason that this model is able to locate unique fitting parameters. Further investigation is necessary in order to determine whether or not this is true.

A potential problem with the gamma MSS model is that low α values are difficult to use in the gamma function. The gamma MSS model is only calibrated for $\alpha \geq 0.35$. Before actually characterizing soils with the gamma MSS model, more sensitivity analysis and model calibration are required.

Since the gamma function is mathematically difficult to use, the lognormal or Weibull density functions might be used instead. The lognormal function has been used by Heyse (1994) and Culver et al. (1997) to describe mass transfer rates. Both the lognormal (equation 10) and Weibull (equation 11) density functions are two-parameter distributions that can assume a wide variety of shapes based on input parameters. These distributions have the potential to be as useful as the gamma distribution described in this thesis.

V. SUMMARY AND CONCLUSIONS

Two problems found in earlier research with the MSS model are examined in this thesis. Both de Venoge's (1996) and Mika's (1997) research find that fitted D_{eff} coefficients depend on sphere sizes. The variations in D_{eff} are not due to the normally distributed sphere masses (and hence sphere sizes), but to the spacing of sampling times during sorption / desorption experiments. Most of the concentration changes occur early in the sorption experiment. These changes must be captured to accurately describe the sorption rate curve and fit model parameters.

When using the MSS model to fit composite particle geometry parameters, nonunique fits are obtained. This is due to limitations of the radial geometry function (equation 8) as the shape factor increases. When the gamma density function (equation 9) is coded into the MSS model, unique fits are obtained for synthetic and natural sorbent data sets.

In the course of determining the answers to these problems, several factors became apparent that merit further attention. First, to improve future sorption experiments, more frequent sampling is needed as the bead size decreases. This will capture earlier portions of the sorption process previously lost due to the faster approach to equilibrium of the high surface area to volume ratio spheres.

The radial geometry MSS model is an improvement over the equivalent sphere model since it preserves the longer path lengths. The gamma MSS model is an even better improvement since it will locate unique *best fit* geometry parameters for composite sorbents, whether that sorbent is natural soil or synthetic material. Continued investigation is needed, however, to calibrate the model for $\alpha < 0.35$ since the shape parameter takes on values

substantially below 0.35 for natural soils. A better algorithm for computing the gamma function may simplify the calibration effort.

Finally, since the gamma function is difficult to evaluate, the lognormal and Weibull density functions should be examined. These functions offer a potential advantage over the gamma function because they are computationally more efficient than the gamma density function. If these functions can also fit unique geometry parameters, characterization of soil types can be accomplished.

APPENDIX A: Borden Soil Data Set

Borden Soil - Gamma MSS model simulation: Run 5

RKD	DEFF	DPATH	RLAM	XSSO	FAST
0.727	0.3390E-10	0.011	2.0	0.0	0.0

1 MEANS FIT PARAMETER, 0 MEANS KEEP IT FIXED

0	1	1	0	0	0
---	---	---	---	---	---

1

0.013481889 0.09779271

CONSTANTS(Ms, VLi, CLi)

1

0.10000E+01	0.10000E+01	0.10000E+01	0.10000E+01	10	
1	0.10000E+03	0.00000E+00	0.00000E+00	0.00000E+00	
1	0.10000E+04	0.00000E+00	0.00000E+00	0.00000E+00	
1	0.10000E+05	0.00000E+00	0.00000E+00	0.00000E+00	
1	0.10000E+06	0.00000E+00	0.00000E+00	0.00000E+00	
1	0.10000E+07	0.00000E+00	0.00000E+00	0.00000E+00	
1	0.20000E+07	0.00000E+00	0.00000E+00	0.00000E+00	
1	0.30000E+07	0.00000E+00	0.00000E+00	0.00000E+00	
1	0.40000E+07	0.00000E+00	0.00000E+00	0.00000E+00	
1	0.50000E+07	0.00000E+00	0.00000E+00	0.00000E+00	
1	0.60000E+07	0.00000E+00	0.00000E+00	0.00000E+00	

1 0.001

EXP	TIME(SEC)	CONCENTRATION(C)
-----	-----------	------------------

1	0.640000000E+03	0.967326343E+00
1	0.190000000E+04	0.944389999E+00
1	0.640000000E+04	0.903672993E+00
1	0.190000000E+05	0.848751038E+00
1	0.550000000E+05	0.778037339E+00
1	0.910000000E+05	0.741218477E+00
1	0.190000000E+06	0.689654505E+00
1	0.280000000E+06	0.665618181E+00
1	0.460000000E+06	0.638607705E+00
1	0.640000000E+06	0.623186839E+00
1	0.820000000E+06	0.613297594E+00
1	0.110000000E+07	0.603763425E+00
1	0.130000000E+07	0.599406350E+00
1	0.180000000E+07	0.592825413E+00
1	0.220000000E+07	0.589753509E+00
1	0.260000000E+07	0.587632942E+00
1	0.350000000E+07	0.584662259E+00
1	0.440000000E+07	0.582938743E+00
1	0.520000000E+07	0.581937766E+00
1	0.610000000E+07	0.581267679E+00
1	0.690000000E+07	0.580767190E+00

APPENDIX B: Mika's (1997) Even Data Set, Condition 5

mharrison TEST FOR MSS model, Run 1: even, two conditions

RKD	DEFF	DPATH	RLAM	XSSO	FAST
9.35	2.0301E-08	0.2453	2.0	0.0	0.0

1 MEANS FIT PARAMETER, 0 MEANS KEEP IT FIXED

0	0	1	0	0	0
---	---	---	---	---	---

9

1 0.1

2 0.1

1 0.25

2 0.25

1.5 0.175

1.574071 0.249172

1.648142 0.323345

1.722213 0.397517

1.796284 0.471690

CONSTANTS(Ms, VLi, CLi)

2

2.02006	20.33937	0.979	1.0	28
---------	----------	-------	-----	----

2.02649	20.40128	0.977	1.0	28
---------	----------	-------	-----	----

1	69840.00	0.56231	0.	0.
---	----------	---------	----	----

1	166560.0	0.45357	0.	0.
---	----------	---------	----	----

1	251460.0	0.41852	0.	0.
---	----------	---------	----	----

1	413160.0	18.38716	20.11721	0.
---	----------	----------	----------	----

1	585060.0	0.36828	0.	0.
---	----------	---------	----	----

1	753960.0	0.36446	0.	0.
---	----------	---------	----	----

1	948360.0	0.41360	0.	0.
---	----------	---------	----	----

1	12777760.	19.07225	20.11115	0.997
---	-----------	----------	----------	-------

1	1361880.	0.41300	0.	0.
---	----------	---------	----	----

1	1468560.	0.40200	0.	0.
---	----------	---------	----	----

1	1549860.	0.43592	0.	0.
---	----------	---------	----	----

1	1632840.	0.45680	0.	0.
---	----------	---------	----	----

1	1793760.	0.37290	0.	0.
---	----------	---------	----	----

1	2921640.	18.01844	20.02739	0.
---	----------	----------	----------	----

1	3022440.	0.39692	0.	0.
---	----------	---------	----	----

1	3102840.	0.40276	0.	0.
---	----------	---------	----	----

1	3193440.	0.38009	0.	0.
---	----------	---------	----	----

1	3275040.	0.40635	0.	0.
---	----------	---------	----	----

1	3371040.	0.46096	0.	0.
---	----------	---------	----	----

1	3448560.	0.44722	0.	0.
---	----------	---------	----	----

1	3610320.	17.57318	20.06768	0.997
---	----------	----------	----------	-------

1	3699960.	0.42443	0.	0.
---	----------	---------	----	----

1	3786060.	0.39373	0.	0.
---	----------	---------	----	----

1	3873060.	0.46827	0.	0.
---	----------	---------	----	----

1	3963060.	0.46509	0.	0.
---	----------	---------	----	----

1	4043460.	0.43136	0.	0.
1	4134660.	0.41749	0.	0.
1	4306260.	0.35215	0.	0.
2	69840.00	0.43149	0.	0.
2	166560.0	0.35314	0.	0.
2	251460.0	0.35427	0.	0.
2	413160.0	18.86931	19.96301	0.
2	585060.0	0.36885	0.	0.
2	753960.0	0.39213	0.	0.
2	948360.0	0.39560	0.	0.
2	1277760.	18.74505	20.28702	0.997
2	1361880.	0.38462	0.	0.
2	1468560.	0.38112	0.	0.
2	1549860.	0.48235	0.	0.
2	1632840.	0.42297	0.	0.
2	1793760.	0.29567	0.	0.
2	2921640.	18.45080	19.91980	0.
2	3022440.	0.38641	0.	0.
2	3102840.	0.42475	0.	0.
2	3193440.	0.39736	0.	0.
2	3275040.	0.40122	0.	0.
2	3371040.	0.41289	0.	0.
2	3448560.	0.48550	0.	0.
2	3610320.	17.45752	20.07969	0.997
2	3699960.	0.43547	0.	0.
2	3786060.	0.40964	0.	0.
2	3873060.	0.42862	0.	0.
2	3963060.	0.42927	0.	0.
2	4043460.	0.36309	0.	0.
2	4134660.	0.42079	0.	0.
2	4306260.	0.43494	0.	0.

1 0.001

EXP	TIME(SEC)	CONCENTRATION(C)
1	166560.0	0.599
1	251460.0	0.570
1	413159.0	0.540
1	413161.0	0.014
1	585060.0	0.209
1	753960.0	0.227
1	948360.0	0.234
1	1277759.	0.239
1	1277761.	0.982
1	1361880.	0.739
1	1468560.	0.676
1	1549860.	0.661
1	1632840.	0.649

1	1793760.	0.641
1	2921639.	0.624
1	2921641.	0.013
1	3022440.	0.201
1	3102840.	0.230
1	3193440.	0.257
1	3275040.	0.280
1	3371040.	0.291
1	3448560.	0.293
1	3610319.	0.302
1	3610321.	0.984
1	3699960.	0.765
1	3786060.	0.721
1	3873060.	0.705
1	3963060.	0.691
1	4043460.	0.686
1	4134660.	0.680
1	4306260.	0.667
1	5085960.	0.651
2	69840.00	0.675
2	166560.0	0.599
2	251460.0	0.571
2	413159.0	0.538
2	413161.0	0.010
2	585060.0	0.211
2	753960.0	0.229
2	948360.0	0.235
2	1277759.	0.241
2	1277761.	0.981
2	1361880.	0.740
2	1468560.	0.686
2	1549860.	0.663
2	1632840.	0.650
2	1793760.	0.642
2	2921639.	0.626
2	2921641.	0.010
2	3022440.	0.202
2	3102840.	0.230
2	3193440.	0.259
2	3275040.	0.280
2	3371040.	0.291
2	3448560.	0.290
2	3610319.	0.301
2	3610321.	0.988
2	3699960.	0.767
2	3786060.	0.724

2	3873060.	0.705
2	3963060.	0.690
2	4043460.	0.689
2	4134660.	0.679
2	4306260.	0.672
2	5085960.	0.653

APPENDIX C: MSS Models

Radial Geometry Function Version

```
C
C Program Testfit
C
C Adapted for batch system experiencing:
C Multisite (series) sorption on soil (variable distribution)
C Liquid-phase added/removed perturbations
C           Simultaneous Fitting multiple experiments
C
C           THIS VERSION CONFIGURED TO CALCULATE
C           SSQ FOR ERROR ONLY
C
C           NUMERICAL SOLUTION
C
C           BY: E. Heyse and D. C. Coulliette
C           University of Florida, 13 Feb 97
C
C           dim scrat = 5*np +np*np +(2+np)*nob
C           signs = 1 means parms cannot change sign
C           P(IPOINT(I)) = VAL(I) == PNAME(I)
C
C           IMPLICIT DOUBLE PRECISION (A-H,O-Z)
C           DOUBLE PRECISION RKD,DEFF,DPATH,RLAM,XSS0,FAST
C           DOUBLE PRECISION XM(10),V(10),PC0(10),SF0(10),XEFT(10),TF
C           DOUBLE PRECISION TBCC(220),VR(220),VA(220),CA(220)
C           DOUBLE PRECISION X(250)
C           DOUBLE PRECISION ANS(0:500001),TIME,CTIME,STOLD,RSLOW
C           DOUBLE PRECISION XIC(501),DELTA(501),FN(501),CL,VS
C           DOUBLE PRECISION XLAM(50),XR(50),SSQ
C           INTEGER FDOMAIN
C           DIMENSION IX(250),Y(250)
C           DIMENSION IFC(220),NEFD(10)
C           CHARACTER*8 PNAME(7)
C           CHARACTER*15 INFIL,OUT1
C           DIMENSION VAL(7),IPOINT(7),IVARY(7)
C           DIMENSION F(250)
C           COMMON /BMOD/XM,V,PC0,SF0,XEFT,NEFD,TBCC,VR,VA,CA
C           COMMON /BMODA/IFLAG,TF
C           COMMON /VALUE/ VAL,IPOINT,IVARY,PNAME,NFIX
C           COMMON /BDAT/ IX,X,NEXP
C           CHARACTER*80 TIT,LIN1,LIN2,LIN3,LIN4
C           NFIX=6
C           PNAME(1)=' Kd '
```

```

PNAME(2)=' Deff '
PNAME(3)=' dpath '
PNAME(4)=' Lambda '
PNAME(5)=' Ss0 '
PNAME(6)=' Fast '
WRITE(*,*) 'NAME OF INPUT FILE?'
READ(5,1111)INFIL
1111 FORMAT(A15)
WRITE(6,*)'NAME OF OUTPUT FILE?'
READ(5,1111)OUT1
OPEN(UNIT=3,FILE=INFIL,STATUS='OLD')
OPEN(UNIT=10,FILE=OUT1,STATUS='NEW')
READ(3,'(A)') TIT
C
C      Read parameters to be fitted
C
C      RKD = partition coefficient, KP,
C      DEFF = Coefficient of Diffusion, D_eff cm^2/sec
C      DPATH = Total diff. path length, d, cm
C      RLAM = shape factor Lambda
C      XSS0 = Initial Concentration in slow soil sites, Sso,  $\mu\text{g/g}$ 
C      FAST = Fraction of equilibrium sorption sites
C
C      READ(3,'(A)') LIN1
C      READ(3,*) RKD,DEFF,DPATH,RLAM,XSS0,FAST
C
C      Read Constants
C
C      FOC = Mass fraction organic carbon on soil, foc
C      XM = Mass of soil in reactor, g
C      V = Volume of solvent in reactor at time zero, mL
C      PC0 = initial concentration in liquid, mg/l
C      SF0 = experiment specific initial concentration in solid
C
C      Note: Intial conc in solid phase = XSS0*SF0(IEXP)
C             if initial sorbed conc is the same for all experiments,
C             make XSS0 = S(t=0) and SF0(IEXP) = 1.0
C             if initial sorbed conc is different for each experiment,
C             make XSS0 = 1.0 and SF0(IEXP) = S(t=0, exp=IEXP)
C
C      NEFD = Number of boundary condition changes
C      IFC = boundary condition number
C      TBCC = time for boundary condition to end
C      XQ = Flow rate, mL/min
C      XCIN = Dimensionless inlet concentration
C      XMR = Mass of reactor, g

```

```

C XKPR = Linear partition coef. on reactor, mL/g
C XKR = 1st order mass transfer rate onto reactor, min^-1
C XFR = Fraction instantaneous sorbing reactor sites
C VS(J) = volume of liquid in rx for BC period j, ml
C VR(J) = volume of liquid removed at end of BC period J, ml.
C VA(j) = volume of liquid added at end of BC period j, ml.
C CA(J) = concentration in liquid added at end of BC period J, mg/l.
C XIC = sorbed concentration in each slow compartment, µg/g
C CL = current liquid concentration, mg/l
C
C      READ(3,'(A)') LIN2
C      READ(3,*) (IVARY(I),I=1,NFIX)
C
C      READ IN HIGH AND LOW values for lambda and R
C
C
C      READ(3,*)NPAIR
C      DO 7 IPAIR=1,NPAIR
C      READ(3,*) XLAM(IPAIR), XR(IPAIR)
7      CONTINUE
      READ(3,'(A)') LIN3
      READ(3,*)NEXP
      NABC=0
      DO 17 I=1,NEXP
      READ(3,*) XM(I),V(I),PC0(I),SF0(I),NEFD(I)
C      READ(3,*) XMR,XKPR,XKR,XFR
      NABC=NABC+NEFD(I)
17      CONTINUE
      DO 6 I=1,NABC
      READ(3,*) IFC(I),TBCC(I),VR(I),VA(I),CA(I)
C          Read numerical parameter
C          IFLAG = 0 for sorbed/liquid concentration
C          IFLAG = 1 for liquid concentration
C          TF = time factor = time of time step/time for mass transfer
C          Try TF = 0.01
      READ(3,*) IFLAG, TF
C
C          Read Data to be fitted
C
C          X = time, seconds
C          Y = observation at time X, see IFLAG.
C
C          XEFT(I) = experiment final time (last observation for each exp.)
C
C
C      READ(3,'(A)') LIN4

```

```

NOB=0
DO 3 I=1,250
READ(3,*,END=4) IX(I),X(I),Y(I)
IF ((I.GE.2).AND.(IX(I).NE.IX(I-1))) XEFT(IX(I-1))=X(I-1)
3 NOB=NOB+1
4 CONTINUE
XEFT(NEXP)=X(NOB)

C
C          Batch model for use with fitting routine TESTFIT
C
C          Set up to handle multiple experiments (10)
C
C          AT THIS POINT WE CYCLE THROUGH VARIOUS VALUES OF
C          PARAMETERS TO CACULATE SSQ BETWEEN OBSERVED
C          AND PREDICTED RESPONSES
C
DO 300 IPAIR2=1,NPAIR
RLAM=XLAM(IPAIR2)
DPATH=XR(IPAIR2)

C
VAL(1)=RKD
VAL(2)=DEFF
VAL(3)=DPATH
VAL(4)=RLAM
VAL(5)=XSS0
VAL(6)=FAST
NFRAC=(RLAM+2.d0)*10+1
IF (NFRAC.LT.50) NFRAC=50
IF (NFRAC.GT.500) WRITE(6,*) 'NFRAC = ', NFRAC
IF (NFRAC.GT.500) WRITE(10,*) 'NFRAC = ', NFRAC
IF (NFRAC.GT.500) WRITE(4,*) 'NFRAC = ', NFRAC

C
C          Loop through each experiment and set up appropriate
C          initial conditions
C
NSUM=0
IT=1
DO 200 IEXP=1,NEXP

C
CL=(PC0(IEXP)*V(IEXP)+XM(IEXP)*XSS0*SF0(IEXP)*FAST)/
     . (V(IEXP)+RKD*XM(IEXP)*FAST)
VS=V(IEXP)

C
C          Input the domain partitioning. Delta(I) is the delta for
C          each compartment.
C

```

```

DO 10 I=1,NFRAC
  DELTA(I)=DPATH/NFRAC
10  CONTINUE
C
C Subroutine INTF generates the F(i)'s by integrating f(delta)
C with RLAM as the shape parameter
C
C Set the initial condition within the immobile zone
C
C CALL INTF(RLAM,DELTA,DPATH,NFRAC,FN)
C
C STOLD is the sum of the S for the diffusion compartments
C
C STOLD=0.0
DO 20 I=1,NFRAC
  XIC(I)=XSS0*SF0(IEXP)*FN(I)*(1.D0-FAST)
  STOLD=STOLD+XIC(I)
20  CONTINUE
C
C Loop through each flow domain
C
C FDOMAIN=1
C TIME=0.0
C Note the final time is X(NOB)
DO WHILE (FDOMAIN.LE.(NEFD(IEXP)+1))
C
C Calculate ANS for beginning of boundary condition
C
C IF (IFLAG.EQ.1) THEN
  ANS(0)=CL
  ELSE
    ANS(0)=(STOLD+FAST*RKD*CL)/CL
  END IF
C
C CTIME is the cumulative solution time
  CTIME=TBCC(FDOMAIN+NSUM)
  IF (FDOMAIN.EQ.(NEFD(IEXP)+1)) THEN
    DO 210 JCOUNT=1,NOB
      IF (IX(JCOUNT).EQ.IEXP) CTIME=X(JCOUNT)
210  CONTINUE
  END IF
C
C Calculate retardation factor for slow sites
C
C RSLOW=(XM(IEXP)*RKD*(1.D0-FAST))/VS
C

```

```

C Calculate the number of time steps for the BC
C
C ITHALF=(CTIME-TIME)*RSLOW*FN(1)*DEFF/(TF*DELTA(1)**2.d0)+1
C ITSTEPS=ITHALF*2
C
C Set minimum value of ITSTEPS
C
C IF (ITSTEPS.LT.100) GOTO 30
C GOTO 35
30 IF ((CTIME-TIME).GT.(XEFT(IEXP)/200.d0)) ITSTEPS=100
C IF ((ITSTEPS.LT.100).AND.((CTIME-TIME).GT.(XEFT(IEXP)/
C 200.d0))) ITSTEPS=100
C
C Warn if number of time steps exceeds array size
C
35 CONTINUE
C IF (ITSTEPS.GT.500000) WRITE(6,*) 'ITSTEPS = ', ITSTEPS
C IF (ITSTEPS.GT.500000) WRITE(10,*) 'ITSTEPS = ', ITSTEPS
C IF (ITSTEPS.GT.500000) WRITE(4,*) 'ITSTEPS = ', ITSTEPS
C IF (ITSTEPS.GT.500000) GOTO 300
C
C FDSOLVE computes the soln from time to ctime for itsteps and
C passes the soln back as array ANS(ITSTEPS)
C
CALL FDSOLVE(TIME,CTIME,ITSTEPS,ANS,XIC,
FN,DELTA,CL,STOLD,VS,IEXP,NFRAC)
C
C INTERP interpolates the soln from FDSOLVE onto the observation
C times and stores the results in array F(nobs)
C
DO WHILE ((X(IT).LE.CTIME).AND.(X(IT).GE.TIME)
.AND.(IX(IT).EQ.IEXP))
CALL INTERP(X(IT),TIME,CTIME,ANS,ITSTEPS,F(IT))
IT=IT+1
END DO
TIME=CTIME
C
C Adjust aqueous volume and new aqueous conc.
C
RFASTV=XM(IEXP)*RKD*FAST+VS
XMADD=VA(FDOMAIN+NSUM)*CA(FDOMAIN+NSUM)
XMREM=VR(FDOMAIN+NSUM)*CL
XNEWM=RFASTV*CL+XMADD-XMREM
CL=XNEWM/(RFASTV-VR(FDOMAIN+NSUM)+VA(FDOMAIN+NSUM))
C CL=(VS*CL+VA(FDOMAIN+NSUM)*CA(FDOMAIN+NSUM)-
C VR(FDOMAIN+NSUM)*CL)/

```

```

C   (VS-VR(FDOMAIN+NSUM)+VA(FDOMAIN+NSUM))
VS=VS-VR(FDOMAIN+NSUM)+VA(FDOMAIN+NSUM)
FDOMAIN=FDOMAIN+1
C
END DO
NSUM=NSUM+NEFD(IEXP)
200 CONTINUE
C
SSQ=0.d0
DO 253 IS=1,NOB
SSQ=SSQ+(Y(IS)-F(IS))**2.d0
253 CONTINUE
WRITE(10,*) RLAM,DPATH,SSQ
300 CONTINUE
C   Output the results
C
CDLC      I=1
CDLC      DO WHILE (I.LT.NOB)
CDLC      WRITE(*,*)I,F(I)
CDLC      I=I+1
CDLC      END DO
CDLC STOP
2222 CONTINUE
STOP
END
C
SUBROUTINE FDSOLVE(TIME,CTIME,ITSTEPS,ANS,XIC,
.FN,DELTA,CL,STOLD,VS,IEXP,NFRAC)
C
C   IMPLICIT NONE
DOUBLE PRECISION RKD,DEFF,DPATH,RLAM,XSS0,FAST
DOUBLE PRECISION XM(10),V(10),PC0(10),SF0(10),XEFT(10),TF
DOUBLE PRECISION TBCC(220),VR(220),VA(220),CA(220)
DOUBLE PRECISION ANS(0:500001),TIME,CTIME,STOLD
DOUBLE PRECISION XIC(501),DELTA(501),FN(501),CL,VS
DOUBLE PRECISION K(501),RES(501),A(501),B(501),RESN,ANS2
INTEGER ITSTEPS,NFRAC
DOUBLE PRECISION SNEW(501),SOLD(501),ST,DELTAT
DIMENSION IFC(220),NEFD(10)
CHARACTER*8 PNAME(7)
DIMENSION VAL(7),IPOINT(7),IVARY(7)
COMMON /BMOD/XM,V,PC0,SF0,XEFT,NEFD,TBCC,VR,VA,CA
COMMON /BMODA/IFLAG,TF
COMMON /VALUE/ VAL,IPOINT,IVARY,PNAME,NFIX
C
DELTAT=(CTIME-TIME)/ITSTEPS

```

```

C
C This version of FDSOLVE solves the compartment
C equations using backward Euler time differencing
C to avoid stability problems. The first-order
C accuracy should be OK since it matches the first-order
C spatial accuracy
C
C Note a Gauss-Seidel solver is used to solve the
C tridiagonal matrix system that results from the
C backward Euler application.
C
C This version of fdsolvem set up for:
C BATCH systems
C Fitting multiple experiments
C
C Set initial conditions from XIC input
C Also use this for initial guess for Gauss-Seidel solver
C
RKD=VAL(1)
DEFF=VAL(2)
DPATH=VAL(3)
RLAM=VAL(4)
XSS0=VAL(5)
FAST=VAL(6)
DO 10 I=1,NFRAC
  SOLD(I)=XIC(I)
  SNEW(I)=XIC(I)
10  CONTINUE
C
NCOUNT=1
C
C Set up constant used to avoid extra calculations
C see Dave's notes
K(1)=2.0*DEFF*DELTAT/(DELTA(1)**2)
DO 20 J=2,NFRAC
  K(J)=2.0*DEFF*DELTAT/((DELTA(J-1)+DELTA(J))*DELTA(J))
20  CONTINUE
C
C Set up matrix constants
DO 30 J=1,NFRAC-1
C Diagonal term
A(J)=1.0+K(J)+FN(J+1)*K(J+1)/FN(J)
30  CONTINUE
C
A(NFRAC)=1.0+K(NFRAC)
DO 40 J=2,NFRAC

```

```

C Subdiagonal term
C B(J)=-K(J)*FN(J)/FN(J-1)
40 CONTINUE
C Note that the super diagonal term is just
C equal to -k(j), j = 1,nfrac-1
C
C DO WHILE (NCOUNT.LE.ITSTEPS)
C
C Gauss-Seidel iteration
C IGITER=0
C RESN=1.0
C DO WHILE((RESN.GT.0.00001).AND.(IGITER.LT.50))
C
C     SNEW(1)=(K(2)*SNEW(2)+SOLD(1)+K(1)*FN(1)
C             *RKD*(1.D0-FAST)*CL)/A(1)
C
C     DO 50 J=2,NFRAC-1
C         SNEW(J)=(SOLD(J)+K(J+1)*SNEW(J+1)-B(J)*SNEW(J-1))/A(J)
C
C 50 CONTINUE
C     SNEW(NFRAC)=(SOLD(NFRAC)-B(NFRAC)*SNEW(NFRAC-1))/A(NFRAC)
C
C Compute residual
C
C     RESN=0.0
C     RES(1)=A(1)*SNEW(1)-K(2)*SNEW(2)-
C             SOLD(1)-K(1)*FN(1)*RKD*CL*(1.D0-FAST)
C
C     RESN=RESN+(RES(1))**2
C
C     DO 60 J=2,NFRAC-1
C
C         RES(J)=A(J)*SNEW(J)-K(J+1)*SNEW(J+1)-
C                 B(J)*SNEW(J-1)-SOLD(J)
C         RESN=RESN+(RES(J)**2)
C
60 CONTINUE
C
C     RES(NFRAC)=A(NFRAC)*SNEW(NFRAC)-
C             B(NFRAC)*SNEW(NFRAC-1)-SOLD(NFRAC)
C     RESN=RESN+(RES(NFRAC)**2)
C     RESN=SQRT(RESN)
C     IGITER=IGITER+1
C
C End Gauss-Seidel loop
C
C END DO

```

```

C
C      Add the sorbed concentrations to update cl
C
C      ST=SNEW(1)
C      DO 70 J=2,NFRAC
C          ST=ST+SNEW(J)
70    CONTINUE
C
C      Update the aqueous concentration using the
C      sorbed concentration solutions
C
C      CL=CL+(XM(IEXP)/(VS+RKD*FAST*XM(IEXP)))*(STOLD-ST)
C      ANS(NCOUNT)=CL
C      ANS2=(ST+FAST*RKD*CL)/CL
C      IF (IFLAG.EQ.0) ANS(NCOUNT)=ANS2
C
C      DO 80 I=1,NFRAC
C          SOLD(I)=SNEW(I)
C          XIC(I)=SNEW(I)
80    CONTINUE
C
C      STOLD=ST
C      NCOUNT=NCOUNT+1
C      END DO
C      RETURN
C      END
C
C      SUBROUTINE INTERP(XT,TIME,CTIME,ANS,ITSTEPS,FR)
C      DOUBLE PRECISION ANS(0:500001),TIME,CTIME,XT,DELTAT
C      DOUBLE PRECISION TIMEC
C      INTEGER ITSTEPS
C
C      DELTAT=(CTIME-TIME)/ITSTEPS
C      NCOUNT=0
C      TIMEC=TIME
C      DO WHILE (XT.GT.TIMEC)
C          TIMEC=TIMEC+DELTAT
C          NCOUNT=NCOUNT+1
C      END DO
C      FR=(ANS(NCOUNT)+ANS(NCOUNT-1))/2.D0
C      FR=(ANS(NCOUNT)-ANS(NCOUNT-1))*(XT-TIMEC+DELTAT)
C          ./DELTAT+ANS(NCOUNT-1)
C      IF (XT.EQ.TIME) FR=ANS(0)
C      IF (XT.EQ.CTIME) FR=ANS(ITSTEPS)
C      RETURN
C      END

```

```

C
SUBROUTINE INTF(RLAM,DELTA,DMAX,NFRAC,FN)
DOUBLE PRECISION DELTA(501),FN(501),RLAM,DMAX
INTEGER NFRAC

C
FAC=(RLAM+1)/(DMAX**(RLAM+1))
I=1
X=0.0
DO WHILE (I.LT.NFRAC)
C Apply Simpson's rule
C FN(I)=DELTA(I)*FAC/6.0*((DMAX-X)**RLAM+
C .4.0*(DMAX-(X+DELTA(I)/2))**RLAM+
C .(DMAX-(X+DELTA(I)))**RLAM)
C FN(I)=(((DMAX-X)**(RLAM+1.D0))-(DMAX-(X+DELTA(I)))***
C .(RLAM+1.D0))/(DMAX**(RLAM+1.D0))
X=X+DELTA(I)
I=I+1
END DO
C FN(NFRAC)=FAC*DELTA(NFRAC)
C FN(NFRAC)=(DELTA(NFRAC)**(RLAM+1.D0))/(DMAX**(RLAM+1.D0))
RETURN
END

```

Gamma Function Version

```
PROGRAM MODEL
C
C This program uses the MSS model for sorption in a batch system
C experiencing liquid phase perturbations and multiple experiments.
C
C THIS VERSION USES A GAMMA DISTRIBUTION
C
C This version calculates the sum of square of error
C between simulated and measured data.
C
C Ed Heyse/Dave Coulliette 3 Dec 97
C Air Force Institute of Technology
C
REAL RKD,DEFF,ALPHA,BETA,XSS0,FAST
DOUBLE PRECISION XM(10),V(10),PC0(10),XEFT(10),SF0(10)
DOUBLE PRECISION TBCC(220),VR(220),VA(220),CA(220)
    DOUBLE PRECISION X(250),XALPHA(200),XBETA(200)
    DOUBLE PRECISION RFASTV,XMADD,XMREM,XNEWM,TF
DOUBLE PRECISION XIC(501),DELTA(501), FN(501)
    DOUBLE PRECISION COBS,DMAX,COBS2
DOUBLE PRECISION STOLD,VS,CL
DOUBLE PRECISION ANS(0:10000001),TIME,CTIME,PTIME
DIMENSION IX(250),Y(250),F(250)
DIMENSION IFC(220),NEFD(10)
DIMENSION VAL(7),IPOINT(7),IVARY(7)
COMMON /BMOD/XM,V,PC0,SF0,XEFT,NEFD,TBCC,VR,VA,CA
COMMON /BMODA/IFLAG,TF
COMMON /VALUE/ VAL,IPOINT,IVARY,NFIX
COMMON /BDAT/ IX,X,NEXP
CHARACTER*80 TIT,LIN1,LIN2,LIN3,LIN4
INTEGER FDOMAIN
CHARACTER*15 INFIL,OUT1
C
C Initialize parameters
C
COBS=3D0.d0
NFIIX=3D6
C
C Names of input and output files
C
WRITE(*,*) 'NAME OF INPUT FILE?'
READ(5,1111)INFIL
1111 FORMAT(A15)
WRITE(6,*)'NAME OF OUTPUT FILE?'
```

```

READ(5,1111)OUT1
OPEN(UNIT=3,FILE=INFIL,STATUS='OLD')
OPEN(UNIT=10,FILE=OUT1,STATUS='NEW')
C
C Read/write input data
C
C READ(3,'(A)') TIT
C WRITE(10,'(A)')TIT
C
C Read parameters to be fitted
C
C RKD = partition coefficient, KP,
C DEFF = Coefficient of Diffusion, D_eff cm^2/sec
C ALPHA = Shape parameter for gamma distribution
C BETA = scaling parameter for gamma distribution
C XSS0 = Initial Concentration in slow soil sites, Sso, ug/g
C FAST = Fraction of equilibrium sorption sites
C
C READ(3,'(A)') LIN1
C READ(3,*) RKD,DEFF,ALPHA,BETA,XSS0,FAST
C WRITE(10,'(A)') LIN1
C WRITE(10,590) RKD,DEFF,ALPHA,BETA,XSS0,FAST
590 FORMAT(6(1X,6E12.5))
C
C Read Constants
C
C XM = Mass of soil in reactor, g
C V = Volume of solvent in reactor at time zero, mL
C PC0 = initial concentration in liquid, mg/l
C SF0 = experiment specific initial concentration in solid
C
C Note: Intial conc in solid phase = XSS0*SF0(IEXP) if initial sorbed
C conc is the same for all experiments, make XSS0 = S(t=0) and
C SF0(IEXP) = 1.0 if initial sorbed conc is different for each experiment,
C make XSS0 = 1.0 and SF0(IEXP) = S(t=0, exp=IEXP)
C
C NEFD = Number of boundary condition changes
C IFC = experiment number
C TBCC = time for boundary condition to end (sec)
C VS(J) = volume of liquid in rx for BC period J, ml
C VR(J) = volume of liquid removed at end of BC period J, ml.
C VA(j) = volume of liquid added at end of BC period j, ml.
C CA(J) = concentration in liquid added at end of BC period J, mg/l.
C XIC = sorbed concentration in each slow compartment,  $\mu$ g/g
C CL = current liquid concentration, mg/l
C

```

```

READ(3,'(A)') LIN2
READ(3,*) (IVARY(I),I=1,NFIX)
C
C READ IN HIGH AND LOW values for alpha and beta
C
READ(3,*)NPAIR
DO 7 IPAIR=1,NPAIR
READ(3,*) XALPHA(IPAIR), XBETA(IPAIR)
7 CONTINUE
READ(3,'(A)') LIN3
READ(3,*)NEXP
NABC=0
C WRITE(10,'(A)') LIN2
C WRITE(10,*) (IVARY(I),I=1,NFIX)
C WRITE(10,'(A)') LIN3
C WRITE(10,*)NEXP
DO 17 I=1,NEXP
READ(3,*) XM(I),V(I),PC0(I),SF0(I),NEFD(I)
C WRITE(10,591) XM(I),V(I),PC0(I),SF0(I),NEFD(I)
NABC=NABC+NEFD(I)
17 CONTINUE
591 FORMAT(1X,4E12.5,I10)
DO 6 I=1,NABC
READ(3,*) IFC(I),TBCC(I),VR(I),VA(I),CA(I)
C WRITE(10,592) IFC(I),TBCC(I),VR(I),VA(I),CA(I)
6 CONTINUE
592 FORMAT(1X,I5,5E12.5)
C
C Read numerical parameter
C IFLAG=0 for sorbed/liquid concentration
C IFLAG=1 for liquid concentration
C TF = time factor = time of time step/time for mass transfer
C Try TF = 0.001
C
READ(3,*) IFLAG,TF
NFRAC1=50
NFRAC2=100
C
C WRITE(10,*) IFLAG,TF,NFRAC1,NFRAC2
CONTINUE
C
C Read Data to be fitted
C
C X = time, seconds
C Y = observation at time X, see IFLAG.
C

```

```

READ(3,'(A)') LIN4
C  WRITE(10,'(A)') LIN4
C  NOB=0
C  DO 3 I=1,250
C  READ(3,* ,END=4) IX(I),X(I),Y(I)
C  IF ((I.GE.2).AND.(IX(I).NE.IX(I-1))) XEFT(IX(I-1))=X(I-1)
3  NOB=NOB+1
4  CONTINUE
C  XEFT(IX(NOB))=X(NOB)
C
C  AT THIS POINT WE CYCLE THROUGH VARIOUS VALUES OF
C      PARAMETERS TO CACULATE SSQ BETWEEN OBSERVED
C      AND PREDICTED RESPONSES
C
C  DO 300 IPAIR2=1,NPAIR
C      ALPHA=XALPHA(IPAIR2)
C      BETA=XBETA(IPAIR2)
C
C  SET VAL PARAMETERS TO PASS TO SUBS
C      VAL(1)=RKD
C      VAL(3)=ALPHA
C      VAL(2)=DEFF
C      VAL(4)=BETA
C      VAL(5)=XSS0
C      VAL(6)=FAST
C
C  CDLC
C      Begin new program for batch solution
C
C      NFRAC is the number of compartments
C
C      NFRAC=(RLAM+2.d0)*10+1
C      IF (NFRAC.LT.50) NFRAC=50
C      IF (NFRAC.GT.500) WRITE(6,*) 'NFRAC = ', NFRAC
C      IF (NFRAC.GT.500) WRITE(10,*) 'NFRAC = ', NFRAC
C
C      Loop through each experiment and set up appropriate
C      initial conditions
C
C      NSUM=0
C      IT=1
C      DO 200 IEXP=1,NEXP
C
C      CL=(PC0(IEXP)*V(IEXP)+XM(IEXP)*XSS0*SF0(IEXP)*FAST)/
C          . (V(IEXP)+RKD*XM(IEXP)*FAST)
C      VS=V(IEXP)

```

```

C
C      Determine upper limit of integration of gamma distribution, DMAX
C
C      SD=-16.661*ALPHA**3.0+38.55*ALPHA**2-31.755*ALPHA+16.066
C      IF (ALPHA.GE.0.59369)SD=-1.2844*LOG(ALPHA)+6.6449
C      DMAX=BETA*(ALPHA+SD*ALPHA**0.5d0)
C
C      Input the domain partitioning. Delta(I) is the delta for each compartment.
C
C      NFRAC=NFRAC1+NFRAC2
C      DO 10 I=1,NFRAC1
C      DELTA(I)=ALPHA*BETA/NFRAC1
10    CONTINUE
C      DO 11 I=NFRAC1+1,NFRAC
C      DELTA(I)=(DMAX-ALPHA*BETA)/NFRAC2
11    CONTINUE
C
C      Subroutine INTF generates the F(i)'s by integrating f(delta)
C      using the gamma distribution
C
C      CALL INTF(ALPHA,DELTA,BETA,NFRAC,FN)
C
C      Set the initial condition within the immobile zone
C
C      STOLD is the sum of the S for the diffusion compartments
C
C      STOLD=0.0
C      DO 20 I=1,NFRAC
C      XIC(I)=XSS0*SF0(IEXP)*FN(I)*(1.D0-FAST)
C      STOLD=STOLD+XIC(I)
20    CONTINUE
C
C      Loop through each flow domain
C
C      FDOMAIN=1
C      TIME=0.0
C      IF (IFLAG.EQ.1) THEN
C      WRITE(10,777)IEXP,TIME,PC0(IEXP)
C      ELSE
C      WRITE(10,777)IEXP,TIME,XSS0*SF0(IEXP)/PC0(IEXP)
C      END IF
C
C      IT=1
C      Note the final time is X(NOB)
C      DO 400 FDOMAIN=1,NEFD(IEXP)+1
C

```

```

C ITSTEPS is the number of time steps per flow domain
C CTIME is the cumulative solution time
C
C Calculate ANS for beginning of boundary condition
C
C IF (IFLAG.NE.0) ANS(0)=CL
C IF (IFLAG.EQ.0) ANS(0)=(STOLD+FAST*RKD*CL)/CL
C
C CTIME=TBCC(FDOMAIN+NSUM)
C IF (FDOMAIN.EQ.(NEFD(IEXP)+1)) CTIME=XEFT(IEXP)
C
C Calculate retardation factor for slow sites
C
C RSLOW=(XM(IEXP)*RKD*(1.d0-FAST))/VS
C
C Calculate the number of time steps for the BC
C
C ITHALF=(CTIME-TIME)*RSLOW*FN(1)*DEFF/(TF*DELTA(1)**2.d0)+1
C ITSTEPS=ITHALF*2
C
C Set minimum value of ITSTEPS
C
C IF ((CTIME-TIME).GT.(XEFT(IEXP)/200.d0)) GOTO 301
C GOTO 302
301 IF (ITSTEPS.LT.100) ITSTEPS=100
302 CONTINUE
C
C Warn if number of time steps exceeds array size
C
C IF (ITSTEPS.GT.10000000) WRITE(6,*) 'ITSTEPS = ', ITSTEPS
C IF (ITSTEPS.GT.10000000) WRITE(10,*) 'ITSTEPS = ', ITSTEPS
C IF (ITSTEPS.GT.10000000) GOTO 2222
C
C FDSOLVE computes the soln from time to ctime for itsteps and
C passes the soln back as array ANS(ITSTEPS)
C
C CALL FDSOLVE(TIME,CTIME,ITSTEPS,ANS,XIC,
C . FN,DELTA,CL,STOLD,VS,IEXP,NFRAC)
C
C Write prediction data to output file
C
C PTIME=TIME
C DELTAT=(CTIME-TIME)/ITSTEPS
C DO 77 II=0,10
C CALCT=PTIME
C IF (II.EQ.0) CALCT=PTIME+1.d0

```

```

C           IF (I.IEQ.10) CALCT=PTIME-1.d0
C           CALL INTERP(CALCT,TIME,CTIME,ANS,ITSTEPS,COBS)
C           WRITE(10,777)IEXP,PTIME,COBS,ITSTEPS
C           WRITE(10,777)IEXP,CALCT,COBS
C           PTIME=PTIME+0.1d0*(CTIME-TIME)
777         FORMAT(1X,I6,2(E20.9))
C           77    CONTINUE
C
C           Calculate predicted values corresponding to observed times
C
C           DO WHILE ((X(IT).LE.CTIME).AND.(X(IT).GE.TIME)
C .AND.(IX(IT).EQ.IEXP))
C           CALL INTERP(X(IT),TIME,CTIME,ANS,ITSTEPS,COBS2)
C               F(IT)=COBS2
C               IT=IT+1
C           END DO
C
C           TIME=CTIME
C
C           Adjust aqueous volume and new aqueous conc.
C
C               RFASTV=XM(IEXP)*RKD*FAST+VS
C               XMADD=VA(FDOMAIN+NSUM)*CA(FDOMAIN+NSUM)
C               XMREM=VR(FDOMAIN+NSUM)*CL
C               XNEWM=RFASTV*CL+XMADD-XMREM
C               CL=XNEWM/(RFASTV-
C               VR(FDOMAIN+NSUM)+VA(FDOMAIN+NSUM))
C               VS=VS-VR(FDOMAIN+NSUM)+VA(FDOMAIN+NSUM)
C
C           Statement 400 = end of do loop for BC change
C
C           400    CONTINUE
C
C           Statement 200 = end of do loop for experiment
C
C           NSUM=NSUM+NEFD(IEXP)
C           200    CONTINUE
C
C           SSQ=0.
C           DO 253 IS=1,NOB
C           WRITE(10,777) IX(IS),X(IS),Y(IS)
C           SSQ=SSQ+(Y(IS)-F(IS))**2.
C
C           253    CONTINUE
C           WRITE(10,254) ALPHA,BETA,SSQ
C           WRITE(6,254) ALPHA,BETA,SSQ
C
C           254    FORMAT(1X,'Alpha = ',E16.5,' Beta = ',E16.5,' SSQ = ',E16.5)

```

```

300  CONTINUE
C
2222 CONTINUE
STOP
END
C
SUBROUTINE INTF(ALPHA,DELTA,BETA,NFRAC,FN)
DOUBLE PRECISION DELTA(501),FN(501),SUM
REAL ALPHA,BETA
INTEGER NFRAC
EXTERNAL FUNC
C
C SUBROUTINE INTF INTEGRATES DISTRIBUTION FUNCTION
C ****GAMMA*****
C FOR EACH COMPARTMENT I
C
SUM=0.d0
I=1
C
C Lower Limit of integration:
C     alpha >= 1: LL = 0
C     alpha < 1: Start from compartment 2, est
C                 compartment 1 from 0.99955 - sum(F2..FN)
C
IF (ALPHA.LT.1.0)X=DELTA(1)
    IF (ALPHA.LT.1.0)I=2
    IF (ALPHA.LT.1.0)GOTO 10
IF (ALPHA.GE.1.0)X=0.d0
C IF (ALPHA.LT.1.0)X=ALPHA*BETA*10.**(-3.8/ALPHA-0.2)
C X=(1.0E-08)*DELTA(1)
10  CONTINUE
DO WHILE (I.LE.NFRAC)
C
X1=X+DELTA(I)
C INTEGRATE FROM X TO X1 USING SUBROUTINE QROMB
C
CALL QROMB(FUNC,X,X1,ALPHA,BETA,T1)
FN(I)=T1
C
SUM=SUM+FN(I)
I=I+1
X=X1
END DO
IF (ALPHA.LT.1.0) FN(1)=0.99955-SUM
RETURN
END

```

```

C
FUNCTION FUNC(X,ALPHA,BETA)
REAL ALPHA,BETA,X
C
T1=EXP(GAMMLN(ALPHA))
FUNC=(BETA**(-ALPHA))*(X**(ALPHA-1))*(EXP(-X/BETA))/T1
RETURN
END
C
SUBROUTINE qromb(func, a, b, alpha, beta, ss)
INTEGER JMAX,JMAXP,K,KM
REAL a, b, func, ss, EPS
EXTERNAL func
PARAMETER (EPS=1.e-7, JMAX=30, JMAXP=JMAX+1, K=8, KM=K-1)
CU USES polint,trapzd
INTEGER j
REAL dss, h(JMAXP), s(JMAXP)
h(1)=1.
do 11 j=1,JMAX
call trapzd(func, a, b, alpha, beta, s(j), j)
if (j.ge.K) then
call polint(h(j-KM),s(j-KM),K,0.,ss,dss)
if (abs(dss).le.EPS*abs(ss)) return
endif
s(j+1)=s(j)
h(j+1)=0.25*h(j)
11 continue
pause 'too many steps in qromb'
END
C (C) Copr. 1986-92 Numerical Recipes Software $!6)$#15[]Nu.
C
SUBROUTINE polint(xa,ya,n,x,y,dy)
INTEGER n,NMAX
REAL dy,x,y,xa(n),ya(n)
PARAMETER (NMAX=10)
INTEGER i,m,ns
REAL den,dif,dift,ho,hp,w,c(NMAX),d(NMAX)
ns=1
dif=abs(x-xa(1))
do 11 i=1,n
dift=abs(x-xa(i))
if (dift.lt.dif) then
ns=i
dif=dift
endif
c(i)=ya(i)

```

```

d(i)=ya(i)
11  continue
y=ya(ns)
ns=ns-1
do 13 m=1,n-1
do 12 i=1,n-m
ho=xa(i)-x
hp=xa(i+m)-x
w=c(i+1)-d(i)
den=ho-hp
if(den.eq.0.)pause 'failure in polint'
den=w/den
d(i)=hp*den
c(i)=ho*den
12  continue
if (2*ns.lt.n-m)then
dy=c(ns+1)
else
dy=d(ns)
ns=ns-1
endif
y=y+dy
13  continue
return
END
C (C) Copr. 1986-92 Numerical Recipes Software $!6)$#15[]Nu.
C
SUBROUTINE trapzd(func,a,b,alpha,beta,s,n)
INTEGER n
REAL a,b,s,func,alpha,beta
EXTERNAL func
INTEGER it,j
REAL del,sum,tnm,x
if (n.eq.1) then
s=0.5*(b-a)*(func(a,alpha,beta)+func(b,alpha,beta))
else
it=2** (n-2)
tnm=it
del=(b-a)/tnm
x=a+0.5*del
sum=0.
do 11 j=1,it
sum=sum+func(x,alpha,beta)
x=x+del
11  continue
s=0.5*(s+(b-a)*sum/tnm)

```

```

        endif
        return
        END
C      (C) Copr. 1986-92 Numerical Recipes Software $!6)$#15()Nu.

        FUNCTION gammln(xx)
        REAL gammln,xx
        INTEGER j
        DOUBLE PRECISION ser,stp,tmp,x,y,cof(6)
        SAVE cof,stp
        DATA cof,stp/76.18009172947146d0,-86.50532032941677d0,
        *24.01409824083091d0,-1.231739572450155d0,.1208650973866179d-2,
        *-.5395239384953d-5,2.5066282746310005d0/
        x=xx
        y=x
        tmp=x+5.5d0
        tmp=(x+0.5d0)*log(tmp)-tmp
        ser=1.000000000190015d0
        do 11 j=1,6
        y=y+1.d0
        ser=ser+cof(j)/y
11      continue
        gammln=tmp+log(stp*ser/x)
        return
        END
C      (C) Copr. 1986-92 Numerical Recipes Software $!6)$#15()Nu.

C      SUBROUTINE FDSOLVE(TIME,CTIME,ITSTEPS,ANS,XIC,
        .FN,DELTA,CL,STOLD,VS,IEXP,NFRAC)
C
C      IMPLICIT NONE
        DOUBLE PRECISION RKD,DEFF,ALPHA,BETA,XSS0,FAST,TF
        DOUBLE PRECISION XM(10),V(10),PC0(10),SF0(10),XEFT(10)
        DOUBLE PRECISION TBCC(220),VR(220),VA(220),CA(220)
        DOUBLE PRECISION ANS(0:10000001),TIME,CTIME,STOLD
        DOUBLE PRECISION XIC(501),DELTA(501),FN(501),CL,VS
        DOUBLE PRECISION K(501),RES(501),A(501),B(501),RESN,ANS2
        INTEGER ITSTEPS,NFRAC
        DOUBLE PRECISION SNEW(501),SOLD(501),ST,DELTAT
        DIMENSION NEFD(10)
        DIMENSION VAL(7),IPOINT(7),IVARY(7)
        COMMON /BMOD/XM,V,PC0,SF0,XEFT,NEFD,TBCC,VR,VA,CA
        COMMON /BMODA/IFLAG,TF
        COMMON /VALUE/ VAL,IPOINT,IVARY,NFIX
C
        DELTAT=(CTIME-TIME)/ITSTEPS

```

```

C
C This version of FDSOLVE solves the compartment equations using backward
C Euler time differencing to avoid stability problems. The first-order accuracy
C should be OK since it matches the first-order spatial accuracy.
C
C Note a Gauss-Seidel solver is used to solve the tridiagonal matrix system
C that results from the backward Euler application
C
C      This version of fdsolvem set up for:
C          BATCH systems fitting multiple experiments
C
C      Set initial conditions from XIC input
C      Also use this for initial guess for Gauss-Seidel solver
C
C      RKD=VAL(1)
C      DEFF=VAL(2)
C      ALPHA=VAL(3)
C      BETA=VAL(4)
C      XSS0=VAL(5)
C      FAST=VAL(6)
C      DO 10 I=1,NFRAC
C      SOLD(I)=XIC(I)
C      SNEW(I)=XIC(I)
10    CONTINUE
C
C      NCOUNT=1
C
C      Set up constant used to avoid extra calculations
C      see Dave's notes
C      K(1)=2.0*DEFF*DELTAT/(DELTA(1)**2)
C      DO 20 J=2,NFRAC
C      K(J)=2.0*DEFF*DELTAT/((DELTA(J-1)+DELTA(J))*DELTA(J))
20    CONTINUE
C
C      Set up matrix constants
C      DO 30 J=1,NFRAC-1
C      Diagonal term
C      A(J)=1.0+K(J)+FN(J+1)*K(J+1)/FN(J)
30    CONTINUE
C
C      A(NFRAC)=1.0+K(NFRAC)
C      DO 40 J=2,NFRAC
C      Subdiagonal term
C      B(J)=-K(J)*FN(J)/FN(J-1)
40    CONTINUE
C      Note that the super diagonal term is just equal to -k(j), j=1,nfrac-1

```

```

C
C      DO WHILE (NCOUNT.LE.ITSTEPS)
C
C      Gauss-Seidel iteration
C      IGITER=0
C      RESN=1.0
C      DO WHILE((RESN.GT.0.00001).AND.(IGITER.LT.50))
C
C      SNEW(1)=(K(2)*SNEW(2)+SOLD(1)+K(1)*FN(1)
C      *RKD*(1.D0-FAST)*CL)/A(1)
C
C      DO 50 J=2,NFRAC-1
C      SNEW(J)=(SOLD(J)+K(J+1)*SNEW(J+1)-B(J)*SNEW(J-1))/A(J)
C
C      50  CONTINUE
C      SNEW(NFRAC)=(SOLD(NFRAC)-B(NFRAC)*SNEW(NFRAC-1))/A(NFRAC)
C
C      Compute residual
C
C      RESN=0.0
C      RES(1)=A(1)*SNEW(1)-K(2)*SNEW(2)-
C      .      SOLD(1)-K(1)*FN(1)*RKD*CL*(1.D0-FAST)
C
C      RESN=RESN+(RES(1))**2
C
C      DO 60 J=2,NFRAC-1
C
C      RES(J)=A(J)*SNEW(J)-K(J+1)*SNEW(J+1)-
C      .      B(J)*SNEW(J-1)-SOLD(J)
C      RESN=RESN+(RES(J)**2)
C
C      60  CONTINUE
C
C      RES(NFRAC)=A(NFRAC)*SNEW(NFRAC)+
C      .      B(NFRAC)*SNEW(NFRAC-1)-SOLD(NFRAC)
C      RESN=RESN+(RES(NFRAC)**2)
C      RESN=SQRT(RESN)
C      IGITER=IGITER+1
C
C      End Gauss-Seidel loop
C
C      END DO
C
C      Add the sorbed concentrations to update cl
C
C      ST=SNEW(1)
C      DO 70 J=2,NFRAC

```

```

ST=ST+SNEW(J)
70  CONTINUE
C
C   Update the aqueous concentration using the
C   sorbed concentration solutions
C
CL=CL+(XM(IEXP)/(VS+RKD*FAST*XM(IEXP)))*(STOLD-ST)
ANS(NCOUNT)=CL
ANS2=(ST+FAST*RKD*CL)/CL
IF (IFLAG.EQ.0) ANS(NCOUNT)=ANS2
C
DO 80 I=1,NFRAC
SOLD(I)=SNEW(I)
XIC(I)=SNEW(I)
80  CONTINUE
C
STOLD=ST
NCOUNT=NCOUNT+1
END DO
RETURN
END
SUBROUTINE INTERP(XT,TIME,CTIME,ANS,ITSTEPS,FR)
DOUBLE PRECISION ANS(0:10000001),TIME,CTIME,XT,DELTAT,FR
DOUBLE PRECISION TIMEC
INTEGER ITSTEPS
C
DELTAT=(CTIME-TIME)/ITSTEPS
NCOUNT=0
TIMEC=TIME
DO WHILE (XT.GT.TIMEC)
TIMEC=TIMEC+DELTAT
NCOUNT=NCOUNT+1
END DO
C
FR=(ANS(NCOUNT)+ANS(NCOUNT-1))/2.D0
FR=(ANS(NCOUNT)-ANS(NCOUNT-1))*(XT-TIMEC+DELTAT)
./DELTAT+ANS(NCOUNT-1)
IF (XT.EQ.TIME) FR=ANS(0)
IF (XT.EQ.CTIME) FR=ANS(ITSTEPS)
RETURN
END

```

APPENDIX D: Details of RSM Procedure for Radial Geometry Function

This appendix details the RSM procedure followed for the radial geometry function version of the MSS model. Mika's (1997) even data set, condition 5 (Appendix B) is used in the MSS model runs to obtain SSE values that form the response surface.

The first minimum bias design of experiments for the radial geometry function is given in Table D-1. These variables are used in the statistical package *SAS JMP™* to obtain the regression function, $\hat{y} = 0.06247 - 0.00709\lambda - 0.04615R$, which is the first-order approximation of the response, SSE.

Table D-1, First 2^2 Factorial Design for Radial Geometry Function

Run #	<u>Coded Variables</u>		<u>Uncoded Variables</u>	Response,	
	X ₁	X ₂	λ	R	SSE
1	$-\sqrt{1/3}$	$-\sqrt{1/3}$	1.2887	0.1683	0.01515
2	$-\sqrt{1/3}$	$\sqrt{1/3}$	1.2887	0.2683	0.07136
3	$\sqrt{1/3}$	$-\sqrt{1/3}$	2.2887	0.1683	0.06888
4	$\sqrt{1/3}$	$\sqrt{1/3}$	2.2887	0.2683	0.00344

The next step is to conduct the gradient search to determine possible directions of improvement. Since an improvement in this case is defined to be a lower SSE, \hat{y} is multiplied by (-1) before taking the partial derivative to obtain the gradient vector. After the gradient vector is divided by its magnitude, the unit gradient vector is obtained, which is also the step size to take for new experiments (in coded units). By use of equation 21, these coded units are transformed to the original variables which are run in the MSS model. The results are shown in Table D-2. Notice that the SSE increases before and after point 4, indicating that this may be the minimum response.

To obtain a better first-order fit, point 4 is used as the center point for another 2^2 factorial design, followed by a gradient search. Table D-3 contains the 2^2 factorial data as well as the gradient search results. Again, notice that point 4 has the minimum response.

Using the data in Table D-3, an augmented first-order design is completed to determine if the fit will be satisfactory. The regression equation is

$$\hat{y} = -0.4195 + 0.2585\lambda + 2.1298\cdot R - 1.2165\cdot \lambda \cdot R$$

with a correlation coefficient (R^2) of 0.7945. This coefficient is probably low due to curvature of the surface. Since a higher R^2 is desired, a second-order response will be fit.

Table D-2, Gradient Search Results

Gradient Vector, \bar{b}	-0.022898	0.751635
Magnitude of \bar{b}	0.7519837	
Unit Gradient Vector	-0.03045026	0.99953628

Run #	Coded Variables		Uncoded Variables		Response SSE
	x_1	x_2	λ	R	
Center Point	0	0	1.5	0.175	0.01930020981
Step Size	-0.03045026	0.99953628	-0.01522513	0.07496522	0.05666088122
Point 1	-0.57735027	-0.57735027	1.21132487	0.13169873	0.01561637710
Point 2	-0.57735027	0.57735027	1.21132487	0.21830127	0.09393009159
Point 3	0.57735027	-0.57735027	1.78867513	0.13169873	0.00478763914
Point 4	0.57735027	0.57735027	1.78867513	0.21830127	0.02344801782
Point 5	-0.03045026	0.99953628	1.48477487	0.24996522	0.13963631887
Point 6	-0.06090052	1.99907257	1.46954974	0.32493044	0.30743289973
Point 7	-0.09135078	2.99860885	1.45432461	0.39989566	0.49175314901
Point 8	-0.12180104	3.99814513	1.43909948	0.47486088	

A central composite design (CCD) is constructed using point 4 from Table D-3 as the center point with one center run. Table D-4 contains the data as input to the *SAS JMP*TM statistical package. With this data, a response surface model is constructed, which results in a second-degree polynomial approximation of the response surface. The summary of fit

information for this model is presented in Table D-5. The correlation coefficient indicates a good fit to the data. This fit is for a small range of λ and R , as can be seen in Table D-4.

Table D-3, Second 2^2 Factorial Design and Gradient Search

Gradient Vector, \bar{b}	0.007094	0.046149
Magnitude of \bar{b}	0.04669106	
Unit Gradient Vector	0.15193487	0.98839051

Run #	Coded Variables		Uncoded Variables		Response SSE
	x_1	x_2	λ	R	
Center Point	0	0	1.78867513	0.21830127	0.0047876391
Step Size	0.15193487	0.98839051	0.13157945	0.08559713	
Point 1	-0.57735027	-0.57735027	1.28867513	0.16830127	0.0151496775
Point 2	-0.57735027	0.57735027	1.28867513	0.26830127	0.0713609895
Point 3	0.57735027	-0.57735027	2.28867513	0.16830127	0.0688815446
Point 4	0.57735027	0.57735027	2.28867513	0.26830127	0.0034405227
Point 5	0.15193487	0.98839051	1.92025459	0.3038984	0.0388629926
Point 6	0.30386974	1.97678102	2.05183404	0.38949553	0.1343904003
Point 7	0.45580461	2.96517152	2.18341349	0.47509266	0.2486271589
Point 8	0.60773948	3.95356203	2.31499294	0.56068978	0.3638264837

Table D-4, CCD for λ , R Response Surface

Run #	Coded Variables		Uncoded Variables		Response, SSE
	X_1	X_2	λ	R	
1	$-\sqrt{1/2}$	$-\sqrt{1/2}$	1.6763	0.2071	0.006034
2	$-\sqrt{1/2}$	$\sqrt{1/2}$	1.6763	0.3295	0.105875
3	$\sqrt{1/2}$	$-\sqrt{1/2}$	2.9010	0.2071	0.053957
4	$\sqrt{1/2}$	$\sqrt{1/2}$	2.9010	0.3295	0.006333
5	-1	0	1.4226	0.2683	0.051296
6	1	0	3.1547	0.2683	0.016846
7	0	-1	2.2887	0.1817	0.052650
8	0	1	2.2887	0.3549	0.056158
9	0	0	2.2887	0.2683	0.003441

Table D-5, Summary Fit data of CCD for λ , R Response Surface

R-Square	0.96936
Adjusted R-Square	0.91829
Root Mean Square Error	0.00971
Mean of Response	0.03917
Observations	9

The fitted model is now

$$\hat{y} = 0.10856 + 0.05997 \cdot \lambda - 1.2371 \cdot R + 0.0400 \cdot \lambda^2 - 0.9831 \cdot \lambda \cdot R + 6.71595 \cdot R^2$$

in the original uncoded units of λ and R . These estimates, the standard errors, and p-values are presented in Table D-6. The p-values indicate that the only significant terms in the model are λ^2 , $\lambda \cdot R$, and R^2 . The effect of removing the other terms is to cause the correlation coefficient (R^2) to decrease. Since these terms are only used to define the response surface, they will be left in the regression model.

Table D-6, λ , R Model Summary Statistics

Term	Estimate	Std Error	t Ratio	p-value
Intercept	0.108556	0.181727	0.60	0.5924
λ	0.059967	0.077913	0.77	0.4975
R	-1.2371	0.868915	-1.42	0.2497
λ^2	0.004005	0.015186	2.64	0.0778
$\lambda \cdot R$	-0.983094	0.129505	-7.59	0.0047
R^2	6.715951	1.518579	4.42	0.0215

A surface plot of this second-order equation can be found in Figure 11. Note how similar the response function plot is to a plot of actual model data over the same region, presented in Figure 12.

The RSM procedure as outlined above is performed with the gamma MSS model for both the even mix data set and the Borden soil data set.

REFERENCES

Ball, W. P. and Roberts, P. V. (1991a)
"Long-Term Sorption of Halogenated Organic Chemicals by Aquifer Material.
1. Equilibrium," *Environmental Science and Technology*, 25 (7): 1223 - 1237.

Ball, W. P. and Roberts, P. V. (1991b)
"Long-Term Sorption of Halogenated Organic Chemicals by Aquifer Material.
2. Intraparticle Diffusion," *Environmental Science and Technology*, 25 (7):
1237 - 1249.

Brewer, R. (1964)
Fabric and Mineral Analysis of Soils, John Wiley & Sons, Inc., New York.

Brusseau, M. L. (1992)
"Nonequilibrium Transport of Organic Chemicals: The Impact of Pore-Water
Velocity," *Journal of Contaminant Hydrology*, 9: 353 - 368.

Brusseau, M. L., Jessup, R. E., and Rao, P. S. C. (1991)
"Nonequilibrium Sorption of Organic Chemicals: Elucidation of Rate-Limiting
Processes," *Environmental Science and Technology*, 25 (1): 134 - 142.

Brusseau, M. L. and Rao, P. S. C. (1989)
"Sorption Nonideality During Organic Contaminant Transport in Porous Media,"
CRC Critical Reviews in Environmental Control, 19 (1): 33 - 99.

Chiou, C. T., Peters, L. J., and Freed, N. H. (1979)
"A Physical Concept of Soil-Water Equilibria for Nonionic Organic Compounds,"
Science, 206: 831 - 832.

Chiou, C. T., Porter, P. E., and Schmedding, D. W. (1983)
"Partition Equilibria of Nonionic Organic Compounds Between Soil Organic
Matter and Water," *Environmental Science and Technology*, 17 (4): 227 - 231.

Connaughton, D. F., Stedinger, J. R., Lion, L. W., and Shuler, M. L. (1993)
"Description of Time-Varying Desorption Kinetics: Release of Naphthalene from
Contaminated Soils," *Environmental Science and Technology*, 27 (12): 2397 - 2403.

Culver, T. B., Hallisey, S. P., Sahoo, D., Deitsch, J. J., and Smith, J. A. (1997)
"Modeling the Desorption of Organic Contaminants from Long-Term Contaminated
Soil Using Distributed Mass Transfer Rates," *Environmental Science and
Technology*, 31 (6): 1581 - 1588.

de Venoge T. P. (1996)

Development of Synthetic Soils for Sorption Mass Transfer Model Validation,
Thesis, Air Force Institute of Technology, Wright-Patterson AFB, OH.

Fetter, C. W. (1992)

Contaminant Hydrogeology, Macmillan Publishing Company, New York.

Goltz, M. N. and Oxley, M. E. (1991)

“Analytical Modeling of Aquifer Decontamination by Pumping When Contaminant Transport is Affected by Rate-Limited Sorption,” *Water Resources Research*, 27 (4): 547 - 556.

Haggerty, R. and Gorelick, S. M. (1995)

“Multiple-Rate Mass Transfer for Modeling Diffusion and Surface Reactions in Media with Pore-Scale Heterogeneity,” *Water Resources Research*, 31 (10): 2383 - 2400.

Hastings, N. A. J. and Peacock, J. B. (1975)

Statistical Distributions, Butterworth & Company, London.

Heyse, E. (1994)

Mass Transfer Between Organic and Aqueous Phases: Investigations Using a Continuously Stirred Flow Cell, Ph.D. Dissertation, University of Florida, Gainesville.

Heyse, E., Dai, D., Rao, P. S. C., and Delfino, J. J. (1997)

“Development of a Continuously Stirred Flow Cell for Investigating Sorption Mass Transfer,” *Journal of Contaminant Hydrology*, 25: 337 - 355.

Karickhoff, S. W. (1981)

“Semi-Empirical Estimation of Sorption of Hydrophobic Pollutants On Natural Sediments and Soils,” *Chemosphere*, 10 (8): 833 - 846.

Karickhoff, S. W. and Morris, K. R. (1985)

“Sorption Dynamics of Hydrophobic Pollutants in Sediment Suspensions,” *Environmental Toxicology and Chemistry*, 4 (1): 469 - 479.

Khuri, A. I. and Cornell, J. A. (1987)

Response Surfaces, Marcel Dekker, Inc., New York.

Konikow, L. F. (1981)

“Role of Numerical Simulation in Analysis of Ground-Water Quality Problems,” *The Science of the Total Environment*, 21: 299 - 312.

Law, A. M. and Kelton, W. D. (1991)
Simulation Modeling and Analysis, Second Edition, McGraw-Hill, Inc., New York.

Mika, D. J. (1997)
Sorption and Desorption Kinetic Modeling of Anthracene Using Paraffin as a Soil Organic Matter Surrogate, Thesis, Wright State University, Fairborn, OH.

Montgomery, D. C. (1976)
Design and Analysis of Experiments, John Wiley & Sons, Inc., New York.

Myers, R. H. and Montgomery, D. C. (1995)
Response Surface Methodology: Process and Product Optimization Using Designed Experiments, John Wiley & Sons, Inc., New York.

Parker, J. C. and Valocchi, A. J. (1986)
“Constraints on the Validity of Equilibrium and First-Order Kinetic Transport Models in Structured Soils,” *Water Resources Research*, 22 (3): 399 - 407.

Pedit, J. A. and Miller, C. T. (1994)
“Heterogeneous Sorption Processes in Subsurface Systems: 1. Model Formulations and Applications,” *Environmental Science and Technology*, 28 (12): 2094 - 2104.

Scow, K. M. and Alexander, M. (1992)
“Effect of Diffusion on the Kinetics of Biodegradation: Experimental Results with Synthetic Aggregates,” *Soil Science Society of America Journal*, 56 (1): 128 - 134.

Schnitzer, M. (1978)
“Humic Substances: Chemistry and Reactions,” *Soil Organic Matter*, (Schnitzer, M. and Khan, S. U., Editors), Elsevier Scientific Publishing Company, Amsterdam, 1 - 64.

Schwarzenbach, R. P., Gschwend, P. M., and Imboden, D. M. (1993)
Environmental Organic Chemistry, John Wiley and Sons, Inc., New York.

Stevenson, F. J. (1982)
“Humus Chemistry: Genesis, Composition, Reactions,” *Humic Substances in Soil, Sediment, and Water*, (Aiken, G. R., McKnight, D. M., Wershaw, R. L., and MacCarty, P., Editors), Wiley Interscience, New York, 1 - 9.

Valocchi, A. J. (1986)
“Effect of Radial Flow on Deviations from Local Equilibrium during Sorbing Solute Transport through Homogeneous Soils,” *Water Resources Research*, 22 (12): 1693 - 1701.

Weber, W. J., McGinley, P. M., and Katz, L. E. (1992)
“A Distributed Reactivity Model for Sorption by Soils and Sediments. 1. Conceptual Basis and Equilibrium Assessments,” *Environmental Science and Technology*, 26 (10): 1955 - 1962.

Wu, S. and Gschwend, P. M (1986)
“Sorption Kinetics of Hydrophobic Organic Compounds to Natural Sediments and Soils,” *Environmental Science and Technology*, 20 (7): 717 - 725.

Young, D. F. and Ball, W. P. (1995)
“Effects of Column Conditions on the First-Order Rate Modeling of Nonequilibrium Solute Breakthrough,” *Water Resources Research*, 31 (9): 2181 - 2192.

Young, T. M. and Weber, W. J. (1995)
“A Distributed Reactivity Model for Sorption by Soils and Sediments. 3. Effects of Diagenetic Processes on Sorption Energetics,” *Environmental Science and Technology*, 29 (1): 92 - 97.

VITA

Maj Mike Harrison was born in Gastonia, N. C., 3 March 1961. He was raised in Northern Virginia and graduated from Robert E. Lee High School in June 1979. After high school, Maj Harrison attended The University of Florida, earning a Bachelor of Science, Environmental Engineering, in December 1984.

After graduation from The University of Florida, Maj Harrison attended Undergraduate Pilot Training at Williams AFB, AZ. His first assignment was flying KC-135Rs at McConnell AFB, KS, from October 1986 to March 1993. While stationed at McConnell AFB, Maj Harrison married the former Tamara Miller. He also earned a master's degree in business from Webster University. His next two assignments were as a KC-135R instructor pilot at Castle AFB, CA and Altus AFB, OK.

Maj Harrison entered the Operations Analysis program at the Air Force Institute of Technology in August 1996. He and Tamara have two children, Dane and Douglas.

After completion of his degree in operations analysis, Maj Harrison will be assigned to the J-5 Branch, Strategic Command, Offutt AFB, NE.

Permanent Address:
4037 Bramley Way
Plano, TX 75093

REPORT DOCUMENTATION PAGE			Form Approved OMB No. 0704-0188
<p>Public reporting burden for this collection of information is estimated to average 1 hour per response, including the time for reviewing instructions, searching existing data sources, gathering and maintaining the data needed, and completing and reviewing the collection of information. Send comments regarding this burden estimate or any other aspect of this collection of information, including suggestions for reducing this burden, to Washington Headquarters Services, Directorate for Information Operations and Reports, 1215 Jefferson Davis Highway, Suite 1204, Arlington, VA 22202-4302, and to the Office of Management and Budget, Paperwork Reduction Project (0704-0188), Washington, DC 20503.</p>			
1. AGENCY USE ONLY (Leave blank)	2. REPORT DATE	3. REPORT TYPE AND DATES COVERED	
	March 1998	Master's Thesis	
4. TITLE AND SUBTITLE		5. FUNDING NUMBERS	
INVESTIGATING SORBENT GEOMETRY RESPONSE SURFACES FROM SORPTION RATE DATA			
6. AUTHOR(S)			
H. Michael Harrison, Major, USAF			
7. PERFORMING ORGANIZATION NAME(S) AND ADDRESS(ES)		8. PERFORMING ORGANIZATION REPORT NUMBER	
Air Force Institute of Technology 2750 P Street WPAFB OH 45433-7765		AFIT/GOA/ENV/98M-01	
9. SPONSORING/MONITORING AGENCY NAME(S) AND ADDRESS(ES)		10. SPONSORING/MONITORING AGENCY REPORT NUMBER	
Capt. Michael Chipley AFOSR/NA 110 Duncan Avenue Suite B115, Bldg 410 Bolling AFB DC 20332-0001			
11. SUPPLEMENTARY NOTES			
Maj. Edward Heyse (Thesis Advisor) 255-3636 X4588 eheyse@afit.af.mil			
12a. DISTRIBUTION AVAILABILITY STATEMENT		12b. DISTRIBUTION CODE	
Approved for public release; distribution unlimited			
13. ABSTRACT (Maximum 200 words)			
Sorption and desorption of hydrophobic organic compounds (HOCs) into soil particles occurs at Air Force contamination sites. Long-term desorption extends clean up time, costing billions. Accurately modeling desorption will reduce costs and improve clean up designs. State of the art models depict soil as uniform spherical particles which lose the effect of longer sorption path lengths. An alternate approach, the multiple sites in series (MSS) model, describes the sorption capacity of a mixture of soil particle sizes and shapes using a composite particle defined by a two parameter statistical distribution. When the MSS model uses a general radial geometry function as the statistical distribution, unique parameters can not be fit to laboratory experimental data. This research employs response surface methodology (RSM) to investigate the nonunique parameter model deficiency. Analysis shows that the response surface for the general radial geometry function is a trough with no unique minimum. A unique minimum is found when the statistical distribution is changed to a gamma distribution.			
14. SUBJECT TERMS			15. NUMBER OF PAGES
Diffusion Coefficient, Sorption, Pollution Abatement, Surface Analysis, Response Surface Methodology			89
			16. PRICE CODE
17. SECURITY CLASSIFICATION OF REPORT	18. SECURITY CLASSIFICATION OF THIS PAGE	19. SECURITY CLASSIFICATION OF ABSTRACT	20. LIMITATION OF ABSTRACT
UNCLASSIFIED	UNCLASSIFIED	UNCLASSIFIED	UL